

# **DEVELOPMENT OF FIRE-RESISTANT HEAVY DENSITY GRIT IRON SCALE AGGREGATE AS GAMMA RAYS SHIELDING MATERIALS**



by

Nabeel Faizan : 19-civil-028  
Muhammad Shoaib : 19-civil-014  
Muhammad Abad Qayyum : 19-civil-003

Project Supervisor

Engr. Inayat Ullah Khan

Lecturer, Civil Department, HITEC University

Project Co-Supervisor

Dr. Muhammad Nasir Ayaz

**CIVIL ENGINEERING DEPARTMENT  
HITEC UNIVERSITY, TAXILA**

June, 2023

**DEVELOPMENT OF FIRE-RESISTANT  
HEAVY DENSITY GRIT IRON SCALE  
AGGREGATE AS GAMMA RAYS  
SHIELDING MATERIALS**

**FINAL YEAR PROJECT REPORT  
SESSION 2019**



**THIS IS SUBMITTED TO THE FACULTY OF  
THE DEPARTMENT OF CIVIL ENGINEERING,  
HITEC UNIVERSITY, TAXILA IN PARTIAL  
FULFILLMENT OF THE REQUIREMENTS  
FOR THE DEGREE OF BACHELOR'S OF  
SCIENCE IN CIVIL ENGINEERING**

**DEPARTMENT OF CIVIL ENGINEERING**

**DEVELOPMENT OF FIRE-RESISTANT  
HEAVY DENSITY GRIT IRON SCALE  
AGGREGATE AS GAMMA RAYS  
SHIELDING MATERIALS**

Submitted by

Nabeel Faizan : 19-civil-028.  
Muhammad Shoaib : 19-civil-014  
Muhammad Abad Qayyum : 19-civil-003

Project Co-Supervisor

Dr. Muhammad Nasir Ayaz Khan  
(Lecturer)

Project Supervisor

Engr Inayat Ullah Khan  
(Lecturer)

Head of Department

Dr. Sabahat Hussain  
(Chairman)

# **DEDICATION**

Dedicated

To

**My Beloved Parents**

## ACKNOWLEDGEMENTS

In the name of Allah, the most merciful and most benefits. First of all our duty is to thank Almighty ALLAH, the creator of whole world, who has blessed us with potential and courage to complete our research task. Another gratitude and countless Darood and Salaams to our greatest and beloved Holy Prophet Hazrat Muhammad ﷺ, for whom this universe has been manifested. I free feel much pleasure in expressing our heartiest gratitude to our ever affectionate, sincere, kind and most respected Supervisor Engr. Inayat Ullah Khan for so patiently guiding us, invaluable suggesting and continuously encouraging us with his precious contributions in completing this thesis. I can never forget that cute smile which he passed while looking at us so affectionately during research working.

I would like to pay the sincerest gratitude to our Co-Supervisor Dr. Muhammad Nasir Ayaz Khan for the provision of research oriented and conductive environment coupled with the appropriate facilities.

I would like deepest thanks to our teachers, Dr. Sabahat Hassan (HOD), and Engr. Yasir Rasheed for their moral support, kind comments and sympathetic attitude during the course of our studies.

We pay profound gratitude to our beloved parents and my sibling, whose sincere prayers, best wishes and loving memories always made us courageous and daring throughout my life. May Almighty ALLAH bless them with good health and prosperous long lives and be a source of prayer for us.

## ABSTRACT

This thesis explores the potential of heavy-density grit scale concrete as a radiation-shielding material at higher temperatures. The study includes the development of methods and covers a complete spectrum of physical qualities of the material between 100C→ to 300C→. The experiment involves preparing samples using different percentages of heavy-density Grit Scale Aggregate (GSA) along with 5% MgO and one normal-weight concrete mix. Several tests were conducted, including mass and density loss, compressive strength, X-ray radiography, scanning electron microscopy, EDX, rebound hammer, and ultrasonic plus velocity tests on pre- and post-heated concrete. The results indicate that the mixes containing 75% heavy-density grit scale aggregate showed significant improvement in shielding characteristics and compressive strength along with the significant contribution of MgO for both pre-and post-heated concrete. This study provides valuable insights into the development of effective radiation-shielding materials for high-temperature applications.

**Keywords.** Fire-resistant, heavy density grit iron scale aggregate, gamma rays shielding materials, elevated temperature.

## LIST OF FIGURES

Figure 1-1 Flow chart and thesis organization .....	9
Figure 2 Flow chart of Concrete density determination program.....	15
Figure 3-1 Gradation Curve of fine aggregates both limits upper and lower .....	18
Figure 3-2 (a) Grit Scale Aggregates with rough and porous Structure .....	20
Figure 3-3 (b) Grit Scale Aggregates with smooth surface .....	20
Figure 3-4 show concrete made with smooth surface GISA .....	21
Figure 3-5 Magnesium Oxide (MgO).....	21
Figure 3-6 (a) EDX analysis of Magnesium Oxide (MgO).....	22
Figure 3-7(b) EDX analysis of Magnesium Oxide (MgO).....	23
Figure 3-8 Show Experimental Program .....	26
Figure 3-9 Experimental diagram of X-ray radiography .....	27
Figure 3-10 Experimental diagram of gamma rays attenuation .....	28
Figure 3-11 Rebound Hammer Test .....	30
Figure 3-12 Ultra-sonic Pulse Velocity Test .....	31
Figure 4-1 Slump test.....	32
Figure 5-1 Slump and Mix Designation .....	39
Figure 5-2(a) Relative density loss against temperature.....	39
Figure 5-3(b) Relative mass loss against temperature .....	40
Figure 5-4 Fresh and hardened density variation with mix designation.....	41
Figure 5-5 Rebound Hammer variation with mix designation .....	41
Figure 5-6 Ultra-sonic Pulse Velocity variation with mix designation .....	42
Figure 5-7 Compressive strength of specimen at various temperatures .....	44
Figure 5-8(a) X-Ray simple (CM 300C→, 75% 300C→).....	45
Figure 5-9(a) Show SEM Analysis at (CM 100C →).....	47
Figure 5.10 (a) linear attenuation coefficient concrete specimen at 300C→.....	60
Figure 5.10(b) linear attenuation coefficient HDC4 at 300C→.....	60
Figure 5.10(c) linear attenuation coefficient CM at room temperature.....	61
Figure 10 (d) linear attenuation coefficient of HDC concrete with temperature...61	61
Figure 10 (e) Mass attenuation coefficient of concrete with temperature.....	61
Figure 5.11(a) Half Value Layer us Temperature.....	63

Figure 5.11(b) Tenth Value Layer us Temperature.....	63
Figure 5.11(c) Mean free path us Temperature.....	63

## LIST OF TABLES

Table 3-1 Chemical and Physical Properties of the Ordinary Portland cement (OPC).....	17
Table 3-2 Physical properties and Chemical composition of normal coarse aggregates and Grit Iron Scale Aggregates .....	19
Table 3-3 Show different designation of concrete mixes .....	24
Table 4-1 Slump values .....	32
Table 4-2 Densities of different concrete .....	33
Table 4-3 Rebound Hammer Test Results.....	33
Table 4-4 Ultra-Sonic pulse Velocity Test Results (m/s).....	34
Table 4-5 Compressive Strength (MPa) .....	35
Table 6-1 Cube volume .....	54
Table 6-2 Quantity of material .....	54
Table 6-3 Material costs .....	55
Table 6-4 Testing expenses .....	55
Table 6-5 Normal weight concrete costs .....	55



## NOMENCLATURE

Abbreviation /  
symbol / Greek  
alphabet

Nomenclature

ASTM	American Society of Civil Engineers
HGSA	Heavyweight Grit Scale Aggregate
HDC	Heavy Density Concrete
NCA	Normal Coarse Aggregates
GSA	Grit Scale Aggregates
MgO	Magnesium Oxide
GISA	Grit Iron Scale Aggregate

EDX	Energy-Dispersive-X-Ray
SEM	Scanning-Electron-Microscopy
HVL	Half-Value-Layer
TVL	Tenth-Value-Layer
CM	100% Normal coarse aggregates
HDC1	25 % Normal Coarse Aggregates and 75% Grit Iron Scale Aggregates
HDC2	25 % Normal Coarse Aggregates and 75% Grit Iron Scale Aggregates
HDC3	50 % Normal Coarse Aggregates and 50% Grit Iron Scale Aggregates
HDC4	75 % Normal Coarse Aggregates and 25% Grit Iron Scale Aggregates

## TABLE OF CONTENTS

### Table of Contents

CHAPTER-1.....	1
1. INTRODUCTION .....	1
1.1 Problem statement:.....	7
1.2 Scope: .....	8
1.3 Research Objectives:.....	8
1.4 Thesis Organization.....	8
2. LITERATURE REVIEW .....	10
2.1 Brief Description .....	10

CHAPTER-3.....	17
3. PROBLEM STATEMENT, METHODOLOGY AND EXPERIMENTAL PROCEDURES.....	17
3.1 Research Methodology.....	17
3.1.1 Research materials .....	17
3.1.2 Mix design.....	23
3.1.3 Mixing, curing and testing specimens.....	24
3.1.4 2.3.1 Concrete design for mechanical strength .....	24
3.1.5 Heating procedure of Concrete specimens .....	24
4. CALCULATIONS AND RESULTS .....	32
4.1 Slump test:.....	32
4.2 Concrete Density Fresh and Hardened .....	32
4.3 Rebound hammer test.....	33
4.4 Ultra-Sonic pulse Velocity .....	34
4.5 Compressive Strength Test .....	35
4.5 Concrete X rays test.....	35
4.6 Scanning electron Microscope (SEM) testing .....	35
4.7 Linear attenuation coefficient .....	36
4.8 Mass attenuation coefficient.....	36
4.9 Half Value Layer, Tenth Value Layer and Mean Free Path.....	37
5. ANALYSIS OF RESULTS.....	38
5.1 Workability and Slump.....	38
5.2 Loss of mass and density .....	39
5.3 Densities .....	40
5.4 Rebound Hammer Test.....	41
5.5 Ultra-sonic Pulse Velocity Test.....	42
5.6 Compressive strength .....	42
5.7 X-Ray radiography core of concrete specimens.....	44
5.8 Scanning electron Microscope (SEM) testing .....	46
5.9 Gamma ray attenuation coefficient.....	48
5.10 Linear attenuation coefficient .....	50

5.11 Mass attenuation coefficient.....	51
5.12 Half Value Layer, Tenth Value Layer and Mean Free Path.....	52
6. BUDGETING AND COSTING OF THE PROJECT .....	54
6.1 Cost per m <sup>3</sup> of heavy density concrete .....	54
7. CONCLUSION .....	57
8. RECOMMENDATIONS AND FUTURE PROSPECTS.....	58

# CHAPTER-1

## 1. INTRODUCTION

Density of heavy weight concrete depends upon specific gravity of aggregate and other specialty of concrete component. Heavy weight concretes are that concrete which specific gravities are above  $2600 \text{ kg/m}^3$  [1]. Mostly high-density coarse aggregates, such as barite, magnetite, hematite, heavy metal oxide, steel slag and steel punching has been used for produced heavy weight concrete for harmful radiation shielding. By using barites and magnetite as a coarse aggregate, the concrete of density more than  $3500 \text{ kg/m}^3$  and  $5000 \text{ kg/m}^3$  can be produced, respectively [2].

Concrete is the most popular protective, structural and building material in average intake in the world  $1\text{m}^3/\text{person}$  per year. Heavyweight concrete finds extensive utilization in nuclear engineering specifically in construction biological shields or shielding walls for various nuclear facilities such as reactor store, nuclear power plants (NPPs), research laboratories, medical facilities and nuclear waste storage. The preference for HWC arises from its natural versatility, affordability, and ease of handling and casting using a variety of techniques.[3].

When adding 2 % of magnesium oxide powder by weight of cement can increase the compressive strength and ultra-sonic velocity at age of 28 days. However, by adding 4% MgO powder form by weight of cement at 28 days it was observed the compressive strength decreased[4].The findings indicate that incorporating MgO in concrete is advantageous for enhancing its strength in the later stages. Once the MgO content surpasses 2 % there is notable increase in the mechanical strength of concrete. However, when the MgO content exceed 5 % the strength begins to decrease. Additionally it should be noted that the MgO expansive agent exhibits expansive properties in the later stages [5]. The utilization of a blend of calcium sulfoaluminate (CSA) and an (MgO) expansive agent

demonstrates a restrain impact on concrete shrinkage and enhances its resistance to cracking[5]. Research conducted in China has indicated that the use of MgO concrete can lead to a significant decrease in construction duration, approximately 50 % less than traditional concrete. It has been discovered that the inclusion of MgO powder in concrete affects its mechanical characteristics, while having minimal impact on its thermal properties. This can be attributed to the irreversibility of the hydration process and the stability of Mg(OH)<sub>2</sub>, resulting in consistent mechanical behavior for MgO concrete[6]. The issues of concrete cracking has long been a concern in the field of engineering. Currently, there are two primary approaches employed to prevent shrinkage cracks in concrete. The first method involves reducing the amount of cement used to mitigate temperature-induced shrinkage or utilizing expansive agents to offset shrinkage. The second approach entails incorporating fibers or additives in the concrete to enhance its ultimate tensile strain. As a solution, concrete containing magnesium expansive agents (MEA) has been developed and successfully utilized for shrinkage compensation in various applications such as dam construction, bridges, road structure, and oil well cement [7]. According to some researchers, concrete can experience temperature increases of up to 250 C. Particularly, the steam temperature in concrete does not go above 150 C. If there is any steam present or if any unintended occurrences occur, a higher temperature may be produced. This phenomenon may occur when the temperature of concrete exceeds 1000C[8].

Due to the enormous urbanization and development taking place all over the world, the need for concrete is rising day by day. One waste product that is produced in enormous quantities worldwide is iron slag. India will produce 24 million tons of IS annually in the future decades [9]. Radiation energy, density, and the element's atomic number all play a role in how well a shielding material can block radiation. Increases in radiation energy cause attenuation to decrease, but Hassan et al. (2015) found that attenuation may be increased by increasing the density of absorbent substances and raising the

atomic number of its constituent. According to Gencel et al. (2011) and Chen et al. (2013), employing the right materials (heavy aggregates) and densifying the concrete can improve the concrete's shielding capabilities. Development of novel materials is required to meet the rising demands for the structure's strength, well-being and protection. Concrete is exposed to gamma radiation in various applications, including nuclear research labs, nuclear reactors, healthcare facilities, and storage casks for nuclear waste (Oto et al., 2015; Yao et al., 2016) [10].

Heavy-weight concrete is made from ferrophosphorus, a material with a reasonably highest specific gravity (5.7 to 6.5 g/cm<sup>3</sup>). The biggest issues with using heavy weight aggregates such as ferrophosphorus is aggregates separation. Due of their substantial specific gravity difference from other components, these particles separate from the concrete. This results in the loss of concrete homogeneity [11].

The MgO concentration of concrete is essential to its stability and capacity for correction. Insufficient MgO content prevents shrinkage correction for concrete from being achieved. If the MgO content is excessively high, the soundness of the concrete will be poor (Wang et al., ...) [12].

Concrete is one of the best materials for radiation shielding from nuclear radiation. It has been shown to be useful in lowering nuclear radiation. Heavy weight concrete which is highly hydrate concrete are consider the most effective varieties of concrete for shielding against gamma rays and attenuating neutrons in radiation application, respectively. They are frequently used in nuclear power plants, nuclear bunkers, radiotherapy megavoltage rooms, the transfer of radioactive sources, and the storage of radioactive waste, according to Akkurt et al. (2012). Operating temperatures for the vast majority of reactor shields are below 100°C. While under abnormal operating conditions (accidents), temperatures could reach 350°C (Engineers, 2003). At high temperatures, a variety of physical, mechanical

and radiation attenuation qualities will alter, and some may even deteriorate[13].

Numerous studies conducted over the past few years have shown that adding admixtures like fly ash, Huck ash, and silica fume can increase concrete's workability, compressive strength, and flexural strength as a result of elevated temperatures. Superplasticizer is a key ingredient that increased workability while using the same amount of water[14].

The two primary secondary particles in proton treatment are neutron and gamma. A continuous component of the gamma energy spectrum starts to drastically decrease above 7MeV. Neutrons have a wide variety of energies, from thermal energy to change beam energy. They don't emit in a uniform way. Low energy neutrons (below 10 MeV) look isotropic due to repeated scattering, whereas high energy neutrons above (10MeV) are obviously forward peaked along the beam [15].

In comparison to conventional concrete of the same strength grade, hematite heavy concrete has a much greater elastic modulus. When metal aggregate is added to the concrete's aggregate, the elastic modulus of the heavy concrete considerably rises[16].

In a previous study, it was shown that using heavy weight concrete as a structural material allowed for a 40% reduction in wall thickness when compared to walls composed of regular concrete.

The improvement of the concrete's shielding characteristics is significantly impacted by the aggregate's high concentration of heavy metals [17].

It looked into why concrete in the Nuclear Power Plants is subjected to high temperature during operation cycles, including internally heat produced by the absorption of the neutrons and gamma rays and heat transferred from the hot reactor systems. Despite the fact that certain category of concrete seem to hold up well, heating makes they loss water through crystallization, weakening them and decreasing their ability to attenuate neutrons[18].



The unmatched benefit of nuclear technology has sped up its development and widespread use. However, it also has some drawbacks, the most serious of which is the high dose radioactive nuclear radiation from variety of source which is extremely harmful and may result in cancer [19].

The radiation shielding and mechanical qualities of that contains fibres made of both lead and steel have been noticeably improved. Several experimental methods, including hot spraying, matrix isolation evaporation condensation, ceramics, laser induced vapor phase reactions and aerosols can be used to create nano-cobalt ferrite ( $\text{CoFe}_2\text{O}_4$ )[20].

Concrete is one of the most widely utilized materials globally, secondly only to water. In this study concrete specimens were exposed to gamma radiation from source like  $^{137}\text{Cs}$  (0.662 MeV) and  $^{60}\text{Co}$  (1.17 and 1.33 MeV). Various parameters such as linear attenuation coefficient (LAC), mass attenuation coefficient (MAC), half-Value layer (HVL), and tenth-value layer (TVL) were analyzed to assess the impact of gamma radiation on the concrete[21].

Currently, Portland cement concrete composites are widely utilized in nuclear and radiation technologies, such as nuclear power plants, irradiation station, research facilities, and radioactive waste storage sites. However, when exposed to radiation environment, these concrete composites experience elevated temperatures, altered linear thermal expansion coefficients and changes in porosity. Consequently, these factors inadvertently lead to increased permeability to air and water According to (Jozwiak-Niedzwiedzka And Brandt.2013).For the duration of a construction, they must have high radiation resistance and mechanical strength (Rosseel et al., 2016) [22].

Numerous studies have shown that one of the substances used most commonly for radiation shielding purposes in a range of institutions, including medical facilities with radioactive sources, particle accelerators, and nuclear power plants, is heavy-weight concrete. Recent studies have concentrated on the use of iron waste products, such as ferritic fume dust, superfine steel dust with a high zinc oxide content, and nanosized magnetite,

to partially substitute Portland cement in the production of radiation-resistant concrete [23].

Specific gravity for heavy weight fine and coarse aggregates is defined as being between 3500 and 7500 kg/m<sup>3</sup>, while unit weight between 2800 and 5600 kg/m<sup>3</sup>. In European mines and Northern

Africa, hematite aggregates (H1), magnetite (M1), and barite (B1, B2, and B3) were utilised. The densities were observed to be 4.20g/cm<sup>3</sup>, 4.05g/cm<sup>3</sup>, 4.18g/cm<sup>3</sup>, 4.80g/cm<sup>3</sup>, and 5.10g/cm<sup>3</sup> for B1, M1, and B3, respectively. A high density of radiation-blocking aggregates was needed for the concrete shield. BaSO<sub>4</sub> content ranged from around 78% in barite aggregates B1 and B3 to almost 90% in aggregate B2, but only slightly higher. Over 85% of the hematite and magnetite aggregate contained ferrum oxide [24].

Chadormelo (Yazd, Iran) provided the magnetite (Fe<sub>3</sub>O<sub>4</sub>) aggregate used in this investigation, which has a specific gravity of 4.58. The coarse aggregate's maximum aggregate size is 25 mm. A method for grading aggregates is described in (ASTM-C637-98a) (ASTM C637-98a and standard S, 2003), the mix design standard for radiation-shielding concrete. By attenuating gamma rays using magnetite aggregates more effectively than with conventional weight aggregates. The results showed that up to 3% of titanium nanoparticles added to cement causes C-S-H gel to form and crystallize during the early stages of hydration, increasing compressive strength and improving penetration resistance. 2019; Nikbin and others. The concrete's internal water vapor pressure increases as the temperature exceeds 100C →. When there are gaps in the concrete, the internal pressure builds up and the concrete may eventually crack. Raising the temperature above 300C → will speed up this process, and if it does so—which is commonly accompanied by a shift in the hue of the concrete from grey to pink—the sculpture may experience catastrophic deformations and irreversible damage [25].

To evaluate the performance of concrete quality Non-destructive testing (NTD) procedures are frequently employed, particularly for post-

construction. For instance, a Rebound hammer and Ultra-Sonic Pulse Velocity have been used to measure the compressive strength and porosity of concrete. Rebound hammer readings increased as concrete's compressive strength increased. The cement and aggregates, level of moist curing and presence of cracks and cavities in concrete all had a considerable impact on ultrasonic pulse velocity values more so than on the measured strengths [26].

In the case of fire in concrete structure as the temperature rises above 100°C → inside the concrete water pressure and voids pressure cause the internal pressure to rise which finally may cause concrete to break. This process will be accelerated by raising the temperature over 300 °C, and if the temperature reached this level which is frequently accompanied by the change in the colour of concrete to pink

It will be a catastrophic scenario for the piece along with permanent deformations. If the temperature rises further and goes above 600°C → the concrete will suffer a severe loss in compressive strength. This reduction may possibly approach 50%, according to experimental testing carried on concrete elements exposed to fire (Kim et al., 1998) [27].

Define the density and composition of aggregates for radiation shielding ACI 304-3R91 (2004) and ASTM C637-14(2019) [28], [29].

## **1.1 Problem statement:**

Concrete is structural and protective materials against ionizing radiation. Gamma rays are used for food preservations, archeological sites, medical field, research laboratories and Nuclear Power Plants (NPP). Gamma rays are harmful to living organisms due to their high penetration power and shorter wavelength. For this purpose, heavy-density concrete is made by heavy-weight aggregates is widely used as a biological shield against harmful gamma rays in NPP, and nuclear waste storage compounds. The cubes will be heat with different temperature such as 28C, 200C and 300C. To cope with this problem, heavy density concrete will be prepared with different percent of grit iron scale and

5% MgO and will be checked for different physical and mechanical properties to quantify the beneficial effect of the grit iron scale and MgO.

## 1.2 Scope:

Food preservations, archeological sites, medical field, research laboratories and Nuclear Power plant (NPP) require protection to avoid health and environmental risks such as ionizing radiation and gamma rays. These rays are harmful to living organisms for this purpose heavy density concrete is made by heavy weight aggregate.

## 1.3 Research Objectives:

- To study heavy weight aggregate pre and past heated heavy weight concrete for physical and mechanical properties
- To study the gamma ray shielding the characteristics pre and past heated heavy density concrete

## 1.4 Thesis Organization

The thesis has been divided into following chapter as given in Figure 01;



Figure 1-1 Flow chart and thesis organization

## CHAPTER-2

### 2. LITERATURE REVIEW

#### 2.1 Brief Description

We can make high performance heavy concrete by using magnetite coarse aggregate along with 10%SF by this compressive strength value exceeds over M60 requirement by 14% after 28 days of curing. High performance concrete can be made with the fine portion of magnetite aggregate which can enhance the shielding efficiency against gamma rays.<sup>1</sup>

In many types of minerals, the tensile and flexural strength is almost similar but the incorporation of fiber steel greatly improves these strengths. By using barites and magnetite as a coarse aggregate, the density of concrete will be more than 3500 kg/m<sup>3</sup> and 5000 kg/m<sup>3</sup> can be produced, respectively.<sup>2</sup>

The thickness of radiation shield can be calculated by using Beer Lambert law techniques as equation  $I = I_0 e^{-ux}$ . Heavyweight concrete (HWC) is used in nuclear engineering in biological shields or shielding walls in a reactor store, nuclear power plant (NPP), research laboratories, medical facilities such as cancer therapy rooms and nuclear waste storage.<sup>3</sup>

According to Mahdi research by adding 2 % of magnesium oxide powder by weight of cement can increase the compressive strength and UPV and there is a reduction in compressive strength when adding 4% Flocrete PC200 to the mixtures where the percentage of reduction at 28 days is 4.14% as compared to reference mixture. UPV of all mixtures increases with age and the results showed that the highest value when adding 2% MgO powder with 4% Flocrete PC200 to the mixture where the percentage increase at 28 days were 59.78% and 21.1 % with respect to reference mixture and mix added 4% Flocrete PC200 respectively. The lowest absorption rate was at 2% addition of MgO powder with 4% Flocrete PC 200 to the mixtures at all ages.<sup>4</sup>

According to Zhang et al.,2021 research when the MgO content exceeds 2%, the mechanical strength of concrete at the later stage increases significantly; however, it begins to reduce when the MgO content is more than 5%. Concrete is the material which is more durable against elevated temperature and fire effects rather than many construction materials.<sup>5</sup>

Concrete with MgOs in china have shown that construction time can be reduced by about 50%, compared to conventional concrete. It has been found that adding MgO powder to concrete will influence the mechanical properties, but have very little effect on thermal properties. Due to because the hydration process is irreversible and the  $Mg(OH)_2$  is stable, the mechanical behavior of MgO concrete is stable. In dam construction, the foundation, lift joint surfaces, and dam abutments provide the external restraints. Dam construction time can be saved through reduction of thermal control measures, reduction or total elimination of transverse. Arch dams can be constructed without transverse or longitudinal contraction joints, saving formwork and thermal protection for the joints surfaces as well as joint grouting work.<sup>6</sup>

Cracking of concrete has always been a problem in the engineering field. At present, there are two main methods to inhibit the shrinkage crack of concrete: One is reducing cement dosage to reduce the temperature shrinkage, or using expansive agents to compensate shrinkage. The second is adding fibers or admixtures in concrete to improve the ultimate tensile strain of concrete The concrete added with magnesium expansive agent (MEA) is then developed and it has been applied for shrinkage compensation in dam concrete, bridge and road structures, oil well cement. The mechanism of MgO hydration can be viewed as a dissolution precipitation process with the controlling and the boundary nucleation and growth model could be used to describe the hydration kinetics of MgO. In cement matrix, the self- expansion of MgO occurs in the confined zone occupied by the initial MgO particles, inducing the expansion and cracking. [Zhang,2021].<sup>7</sup>

In civil engineering projects concrete is subjected to different temperatures to extract better results of concrete. According to some researchers, concrete can experience temperature increases of up to 250 C. Particularly, the steam temperature in concrete does not exceed 150 C. If there is any steam present or if any unintended occurrences occur, a higher temperature may be produced. This phenomenon may occur when the temperature of concrete exceeds 1000C.8

The world is running out of NFA and demand of sand increasing day by day. So, the need for concrete is rising day by day. One waste product that is produced in enormous quantities worldwide is iron slag. India is producing 24 million tons of IS annually in the future decades. We can make environmental friendly concrete by replacing NCA with RCA.9

Radiation energy, density, and the element's atomic number all play a role in how well a shielding material can block radiation. Increases in radiation energy cause attenuation to decrease, but Hassan et al. (2015) found that attenuation may be increased by increasing the density of absorbent material and the atomic number of the elements in the material. According to Gencel et al. (2011) and Chen et al. (2013), employing the right materials (heavy aggregates) and densifying the concrete can improve the concrete's shielding capabilities. Development of novel materials is required to meet the rising demands for the structure's strength, durability, safety, and security. Concrete is exposed to gamma radiation in various applications, including nuclear reactors, nuclear research labs, healthcare facilities, and storage casks for nuclear waste.

The HWUHPC mixtures, evaluated under the present work, possess enhanced mechanical properties and high radiation shielding that provide safety to the structural elements in a power plant against structural failure as well as shielding of nuclear radiation in case of earthquakes or accidental loading. 10

Heavy-weight concrete is made from ferrophosphorus, a material with a reasonably high specific gravity (5.7–6.5 g/cm<sup>3</sup>). The biggest problem with using heavy aggregates like ferrophosphorus is aggregate separation. Due of

their substantial specific gravity difference from other components, these particles separate from the concrete. This results in the loss of concrete homogeneity. We can make concrete better by adding different components to improve the compressive strength. The most effective factor in increasing the compressive strength was ferrophosphorus, followed by Nano silica, and then steel powder, respectively when ferrophosphorus content increases the compressive strength generally increases. The complete replacement of normal aggregate with ferrophosphorus, in similar content of other materials increased the compressive strength by 48% at the concrete age of 28 days.<sup>11</sup>

The yield stress and plastic viscosity of cement pastes containing 6wt% MEA increase by 143% and 128% respectively, with strength grade increasing from Grade 30 to Grade 45. The yield stress and plastic viscosity of MEA content increasing from 0 to 8wt%. 1wt% MEA replacement of cement makes the yield stress and thus plastic viscosity increasing by 7% and 3% respectively. The MgO concentration in concrete is essential to its stability and capacity for correction. Insufficient MgO content prevents shrinkage correction for concrete from being achieved. If the MgO content is excessively high, the soundness of the concrete will be poor.<sup>12</sup>

Concrete is one of the best materials for radiation shielding from nuclear radiation. It has been shown to be useful in lowering nuclear radiation. Heavy weight concrete (HWC) and highly hydrated concrete are the best types of concrete used in radiation shielding for gamma ray and neutron attenuation, respectively. They are frequently used in nuclear power plants, nuclear bunkers, radiotherapy-mega voltage rooms, the transfer of radioactive sources, and the storage of radioactive waste, according to Akkurt et al. (2012). Operating temperatures for the vast majority of reactor shields are below 100 °C. While under abnormal operating conditions (accidents), temperatures could reach 350 °C (Engineers, 2003). At high temperatures, a variety of physical, mechanical, and radiation attenuation qualities will alter, and some may even deteriorate.<sup>13</sup>



Numerous studies conducted over the past few years which shows that adding admixtures like fly ash, Huck ash, and silica fume can increase concrete's workability, compressive strength, and flexural strength as a result of elevated temperatures. Superplasticizer is a key ingredient that increase the performance of concrete and it also reduce the cement consumption during construction on concrete or buildings and bridges. Two types of superplasticizers were used to make concrete workable such as viz., sulphonated naphthalene formaldehyde(SNF) based and polycarboxylic ether (PCE). Before using superplasticizer in concrete durability test was also conducted on concrete by evaluating the percentage water absorption for different grades of concrete with and without superplasticizer.<sup>14</sup>

The two primary secondary particles in proton treatment are neutron and gamma. A continuous component of the gamma energy spectrum starts to drastically decrease above 7 MeV. Neutrons have a wide variety of energies, from thermal energy to beam energy. They don't emit in a uniform way. Low energy neutrons (below 10 MeV) look isotropic due to repeated scattering, whereas high energy neutrons (above 10 MeV) are obviously forward-peaked along the beam axis.

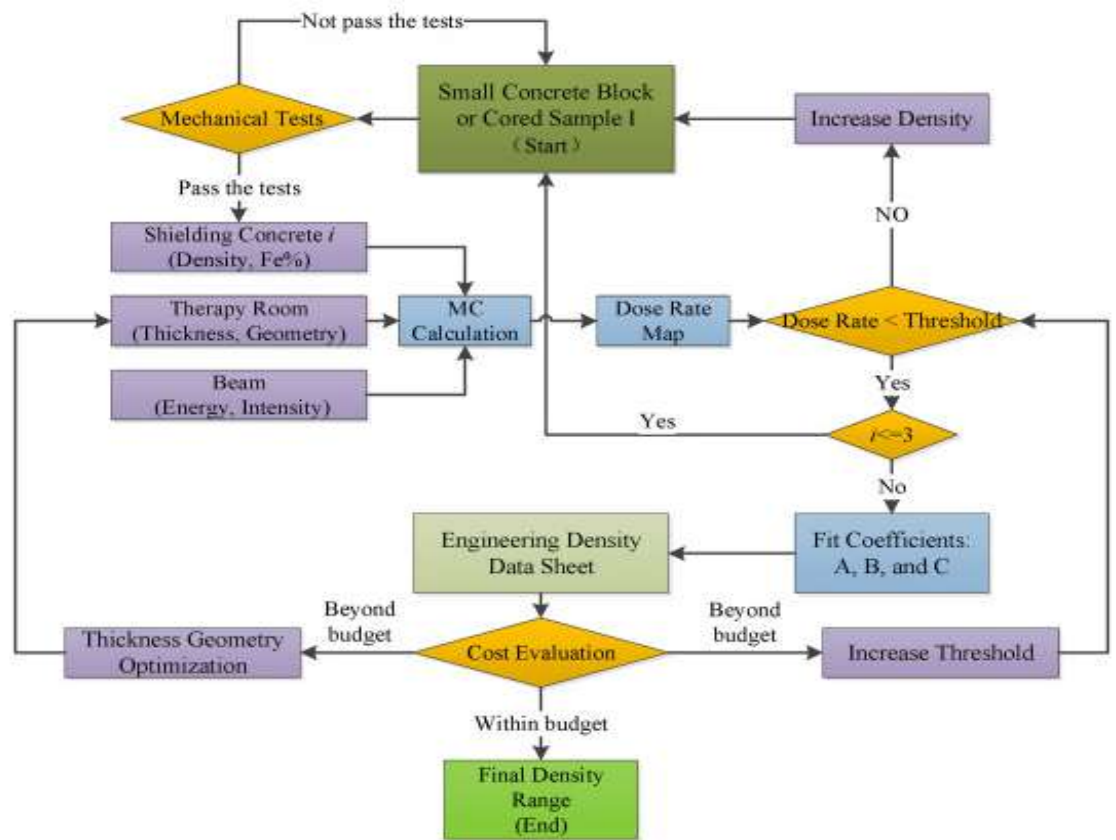


Figure 2 Flow chart of Concrete density determination program

The compressive strength of concrete on 14<sup>th</sup> day after pouring is 35.7Mpa. its density ranges from 3.65g/cm<sup>3</sup> to 4.14g/cm<sup>3</sup> and its iron mass content ranges from 35.78% to 60.38% from 12 cored measurements. Mixing impurities can be the reason leading to this nonuniform element disturbed the density. So the density and element composition should be balanced in the design on concrete.15

In comparison to conventional concrete of the same strength grade, hematite heavy concrete has a much greater elastic modulus. When metal aggregate is added to the concrete's aggregate, the elastic modulus of the heavy concrete considerably rises. So the addition of hematite in concrete can increase the unit weight (density) so that the smaller thickness of concrete is required to provide shielding radiation. After 30 freeze thaw cycles the plain concrete loses 21.35 of its compressive strength while the composite containing 10% losses of hematite and 7.8% of the strength.16

In a previous study, it was shown that using heavy weight concrete as a structural material allowed for a 40% reduction in wall thickness when compared to walls composed of regular concrete.

The improvement of the concrete's shielding characteristics is significantly impacted by the aggregate's high concentration of heavy metals.<sup>17</sup>

## CHAPTER-3

### 3. PROBLEM STATEMENT, METHODOLOGY AND EXPERIMENTAL PROCEDURES

#### 3.1 Research Methodology

##### 3.1.1 Research materials

As per standards specification ASTM C-150 ordinary Portland cement (OPC) was utilized in this research of brand named as “Dewan Cement” having specific gravity of 3.14 [30]. For color and smoothness cement was actually observed substantially. Table 3.1 contains the data regarding cement properties physical as well chemical [31].

Table 3-1 Chemical and Physical Properties of the Ordinary Portland cement (OPC)

Chemical Composition	Values (%)	Physical Properties	Values
<u>CaO</u>	63	Specific gravity (g cm <sup>-3</sup> )	3.14
SiO <sub>2</sub>	22	Average particle size(μm)	19
<u>AlO</u>	9.58	Blaine (m <sup>2</sup> /kg)	160 Min
Mg <sub>2</sub> O <sub>3</sub>	2.91	Initial setting time	1 hour
Fe <sub>2</sub> O <sub>3</sub>	3	Final setting time	600 Max (10 hour)
SO <sub>3</sub>	1.75	Consistency (%)	
Na <sub>2</sub> O	0.5	-	

According to ACI-304 and ASTM C9 Section 2-3 refers to the excellence of water utilized in heavy weight concrete and water should be free any other contaminant [25]. When concrete is to be mixed the main concerns are bleeding

and segregation. Lawrancepur's sand (fine aggregates) with fineness modulus 2.6 were used during this research. Fig. 3.1 shows the gradation curve of fine aggregates both limits upper and lower.

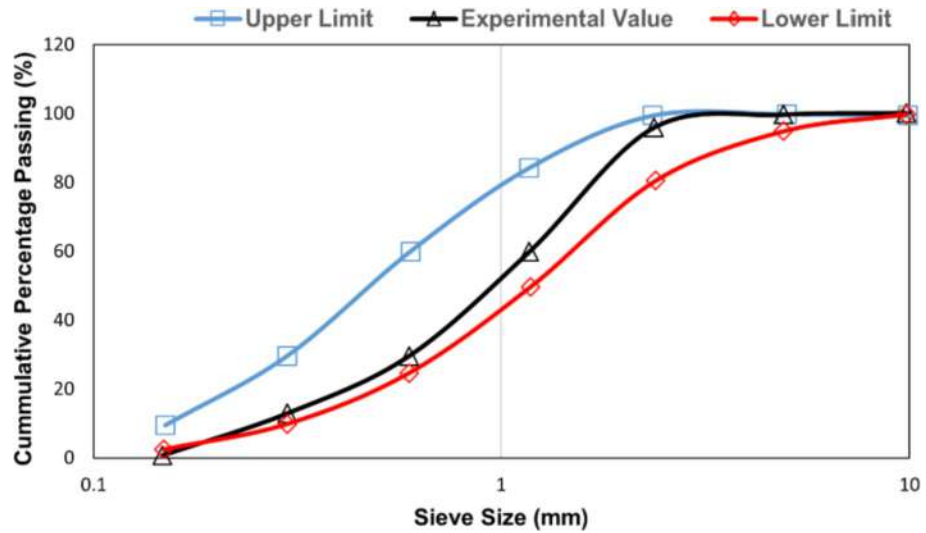


Figure 3-1 Gradation Curve of fine aggregates both limits upper and lower

Range of heavy weight aggregates was same as the normal weight aggregate as per standards specification (ASTM C33) [32]. This research utilized normal weight aggregate (NWA) having density of 2400kg/m<sup>3</sup> and water absorption 1.2 % was collected from Margalla Hills. Aggregates were classified in three groups. Table 3.2 refers to the physical as well as chemical properties of aggregates.

Table 3-2 Physical properties and Chemical composition of normal coarse aggregates and Grit Iron Scale Aggregates

Chemical composition	NWA	GSA	Physical properties	NWA	GSA
	Values %	Values %		Values %	Values %
Fe	0.44	95%	Specific gravity	2.4	6.63
Si	43.21	1.67%	Bulk density ( $\text{g cm}^{-3}$ )	1.44	3.96
Mn	0.03	1.20%	Hardness (Mohs Scale)	7	9
C	-	1.20%	Melting point °C	-	1430
Cu	0.04	Less than 0.2%	Colour	light grey	Grey
Ni	0.06	less than 0.15%	Shape	Angular	Angular + grit
Mg	4.69	-	Water absorption % (smooth)	1.20	0.9
Ca	8.67	-	Water	-	1.3

These gatherings comprise of 5-9mm, 5-16mm, and 5-25mm coarse totals. Various concrete Blends were ready from these gatherings. With fine aggregate with 2.6 fineness modules and 1.7% of water absorption according to as per standards specification were used by ASTM C-637[33]. ASTM (C638.20) says that heavy weight aggregates have higher density than naturally occurring aggregates [34, p. 638] . Grit scale (GSA) aggregates were used as heavy weight aggregates having specific gravity of 3.91. The GISA were collected from Heavy-Mechanical-Complex (HMC) Taxila, Pakistan. The GISA was truly surveyed, eliminating other harmful components, dirt and iron Pellets. Sieve analysis was done on Grit Iron Scale Aggregates (GISA), and coarse totals somewhere in the range of 5 and 25mm were obtained.

During performing testing it was observed that two kinds of coarseness scale

which are strong with a cleaned surface and permeable with an unpleasant surface as displayed in Fig 3.2 (a) and 3.2(b) separately.



Figure 3-2 (a) Grit Scale Aggregates with rough and porous Structure



Figure 3-3 (b) Grit Scale Aggregates with smooth surface

The permeable aggregates water absorption 1.3% was most important than non-permeable ones 0.9%. The chemical and actual properties of GISA are enlisted in Table 3.2. At first, because of water absorption low, the Blends ready with strong and smooth totals have great work-capacity. During casting and demolding there have no adhesion between paste and aggregates was observed. Second, the aggregates towards settle down in a mix, resulting in aggregate clusters, as illustrated in Fig 3.4, because of its heavy density and smooth surface. Because utilizing only porous aggregates increased water demand, the trial mixes were discarded and a mixture of both smooth and porous aggregates was employed.



Figure 3-4 show concrete made with smooth surface

GISA

The magnesium oxide (MgO) with density 3535.71 kg/m<sup>3</sup> collected from Karachi, Pakistan shown in Fig.3.5.



Figure 3-5 Magnesium Oxide (MgO)

EDX analysis was done on magnesium oxide MgO at Centralized-Resource Laboratory (CRL) University of Peshawar (UOP) Pakistan, it shown maximum amount of magnesium oxide as shown in 3.6 (a) and 3.6 (b).



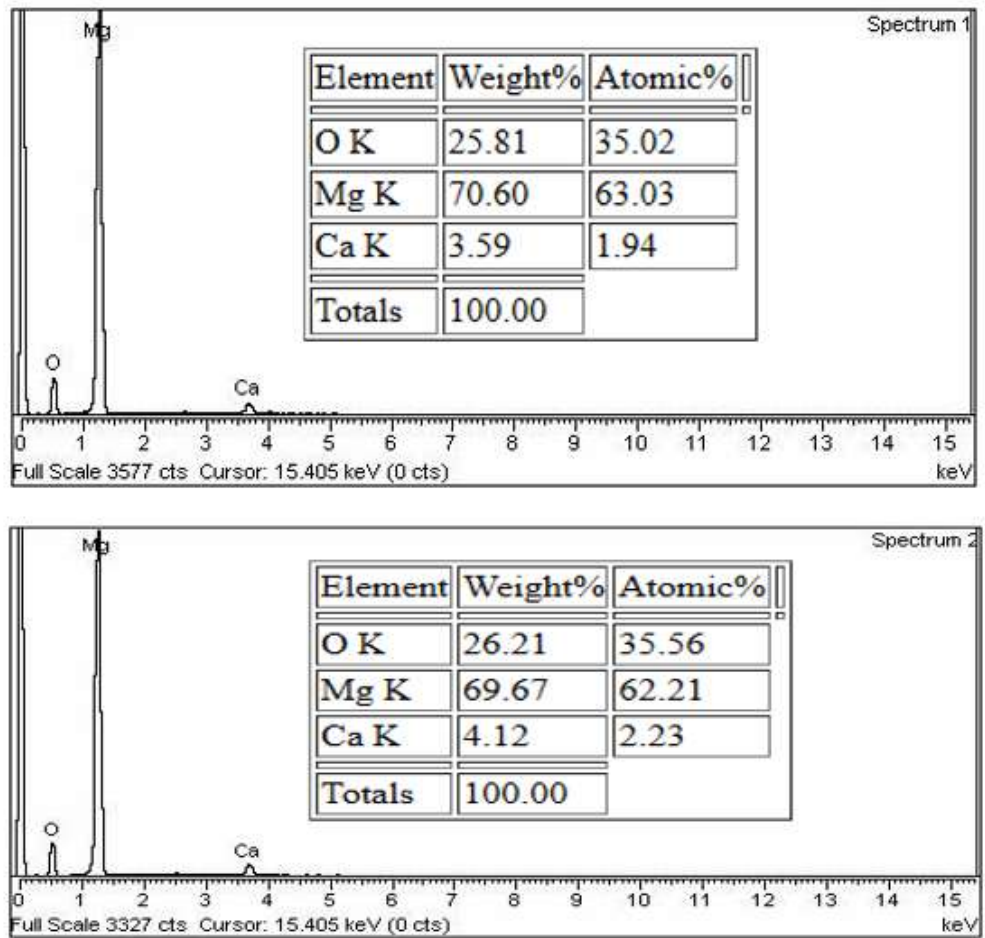


Figure 3-6 (a) EDX analysis of Magnesium Oxide (MgO)

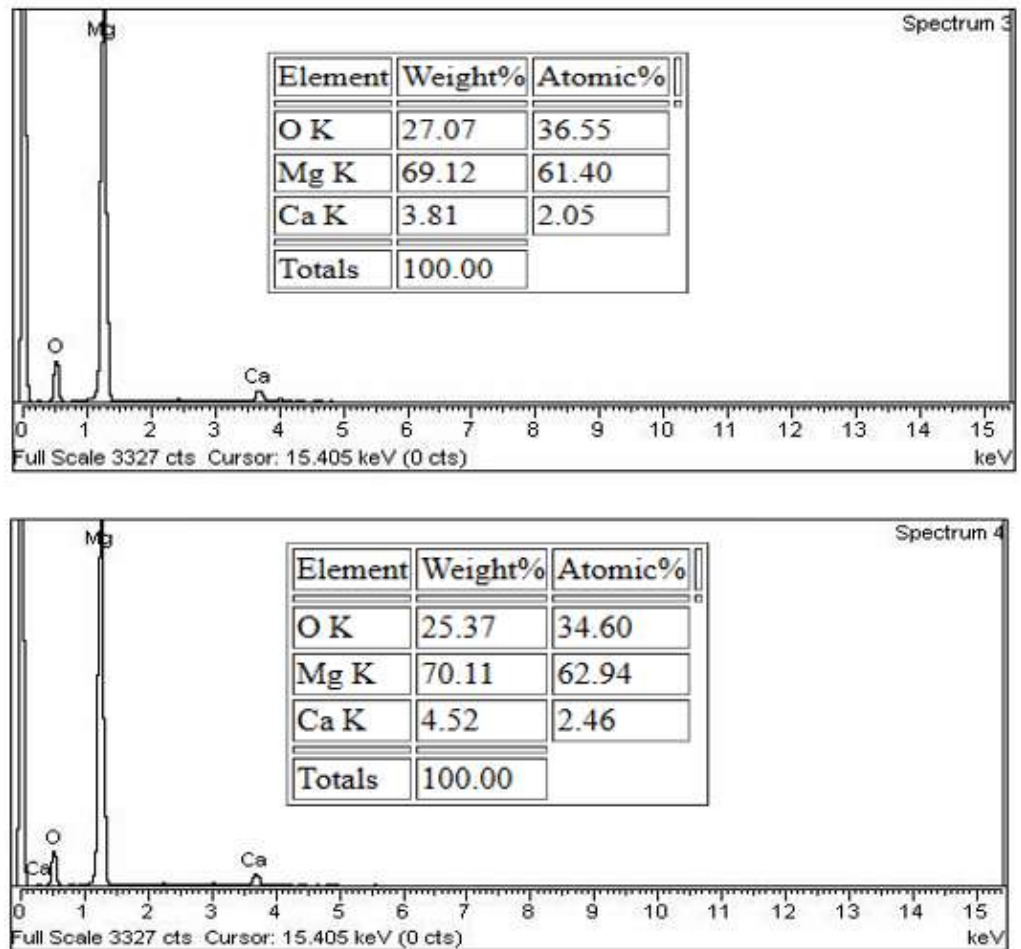


Figure 3-7(b) EDX analysis of Magnesium Oxide (MgO)

### 3.1.2 Mix design

Totally five mix were designed including comparison purpose controlled mixes CM and other four Heavy density Grit Iron Scale concrete (HDC1, HDC2, HDC3, HDC4) were prepared using constant to water cement ratio (w/c)0.4 constant throughout all mixes in this study . Where HDC1 means Heavy density concrete which contain 25 % Grit iron Scale Aggregates and 75 % normal weight Aggregates. Other mixes are show in Table 3.3. Heavy weight concrete mixes can be proportioned utilized according to American Concrete Institute Method (ACI) of absolute volumes developed for normal concrete[1].

Table 3-3 Show different designation of concrete mixes

Concrete type	Aggregate ratio	w/c	Water (kg/m <sup>3</sup> )	Cement (kg/m <sup>3</sup> )	Fine aggregate (kg/m <sup>3</sup> )	Coarse aggregate (kg/m <sup>3</sup> )	GSA (kg/m <sup>3</sup> )	MgO (kg/m <sup>3</sup> )
CM	100% Limestone aggregates (5-25 mm)	0.4	173.93	434.83	821.34	1123.3	-	-
HGS1	25% GSA + 75% Limestone (5-25 mm)	0.4	173.93	413.08	205.33	842.47	280.83	21.74
HGS2	50% GSA + 50% Limestone (5-25 mm)	0.4	173.93	413.08	410.67	561.65	561.65	21.74
HGS3	75% GSA + 25% Limestone (5-25 mm)	0.4	173.93	413.08	611	280.82	842.47	21.74
HGS4	100 % GSA (5 - 25 mm)	0.4	173.93	413.08	-	-	1123.3	21.74

The content of cement same throughout all the mixes which was 11.07 kg. MgO 5% constant in all mixes which was 77.014 g. however, quantity and size of coarse were different for design mixes. CM have 100% coarse aggregate groups (5, 9, 16 and 25mm). Where HDC1 have NWA 75% which was mixture of different groups (5, 9, 16 and 25mm), and HDC1 show that 25 % GSA by exchange NWA and so on.

### 3.1.3 Mixing, curing and testing specimens

#### 3.1.4 2.3.1 Concrete design for mechanical strength

The mixing procedure of Heavy density concrete was same like normal weight concrete only difference of mixing time which was less for Heavy weight due to avoid segregation phenomena. Total 40 of cubes for five separate mixes with same dimension (150mm x150mm x150mm) were casted. Slump test were performed each mixes during the casting as per standards ASTM C-143/C-143M-20 [35]. Also noted the wet density all mix as per standards specification C-948-81 [36]. Then cubes were cured in water tank for 28 days under the condition (temperature 25C→±5C→).

### 3.1.5 Heating procedure of Concrete specimens

After the curing 28 days, for heating the specimens were weighted and placed in the heating Oven .before the mass constant the cubes were dried an Oven at 110C $\rightarrow$  for 24hours to remove any extra water. For apparent density again weighted of specimens. Specimens were subjected to heating at various temperature (100C $\rightarrow$ , 200C $\rightarrow$ , and 300C $\rightarrow$ . ) using separate ovens .there are two type of furnaces were employed an electrically operated box- type air furnace( measuring 500mm x 600mm x1200mm) and other a nature gas-operated heating furnace ( measuring 600mm x 600mm x1200mm). The furnace were designed to achieve a maximum desired temperature of 300C $\rightarrow$  with a tolerance of  $\pm 20$ C $\rightarrow$ . The furnace were equipped with trolleys for convenient loading from the front. The box-type air furnace utilized fibrous insulation materials on the sides and insulated palates on the base to ensure proper insulation. The forced ventilator was installed to circulate air from the surrounding atmosphere into the furnace. The entire process from loading to heating and unloading was controlled by a programmable controller.

The loading rate was rise  $3 \pm 2$ C/min temperature. For temperature 100C $\rightarrow$ , 200C $\rightarrow$  and 300C $\rightarrow$ the heating process was carried out in 24hours. The loading and unloading of specimens, heating and cooling was done in one day then open the doors to bring specimens to room temperature. According to the criteria the furnace was minimum distance between two specimens was equal to their diameter for specimens. Then after the heating procedure the specimens were again weighted mass and density loss. Then specimens were tested against the compression test as per standards specification ASTM C39/39 M [37]. Graphically procedure shown in Fig.3.8.

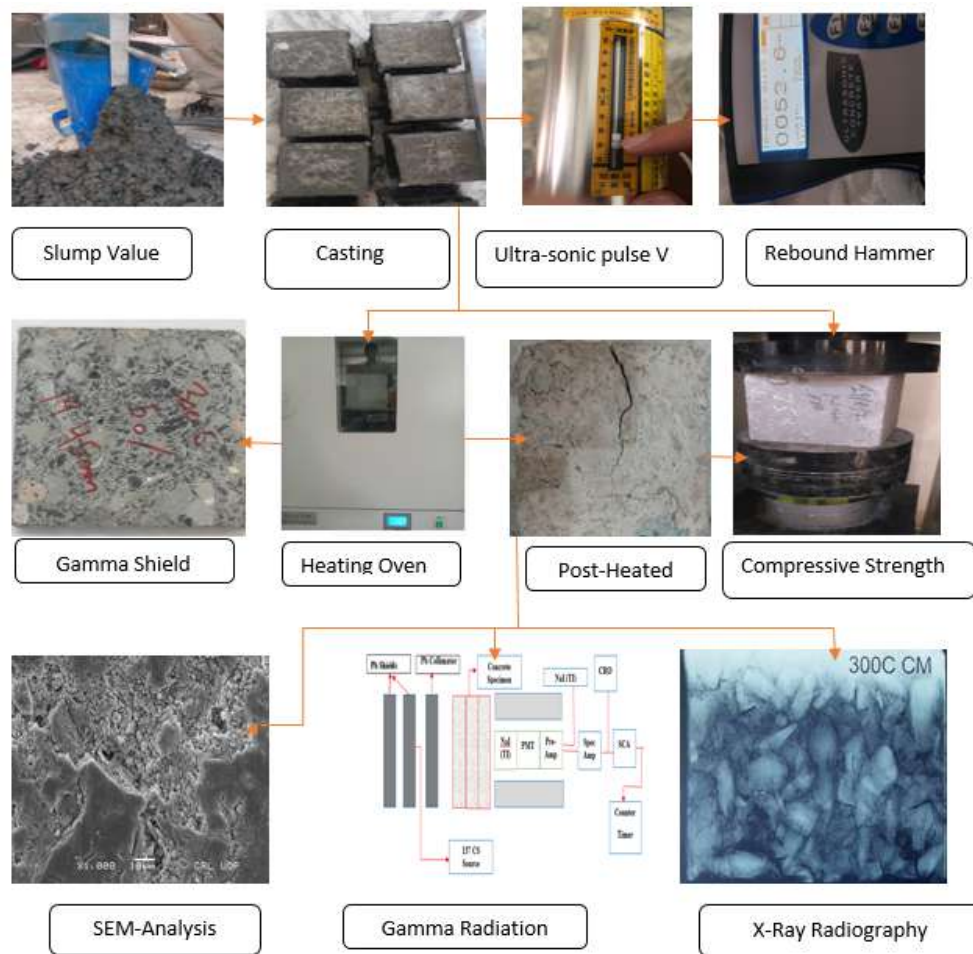


Figure 3-8 Show Experimental Program

### 2.3.3 Radiography of X-ray concrete core imaging

It is traditional and very effective method to find the concrete core or internal specification. Its show obtained precise and visualization of cracks gas voids, air pockets and other type of pores within the simple[38]. For X-Ray radiography the pre-and post-heated specimens with dimensions (150mmX150mm X20mm) were sent to Metallographic Testing Lab (MLT), Non-destructive Testing (NTD) in Wah International Hospital (WIH), Pakistan. This test were conducted on D7 film with radiation exposure of 1 minute. To achieve optimal results, a lead table was utilized to position X-ray film which was then placed over the surface Fig 3.9 represent X-ray radiography.

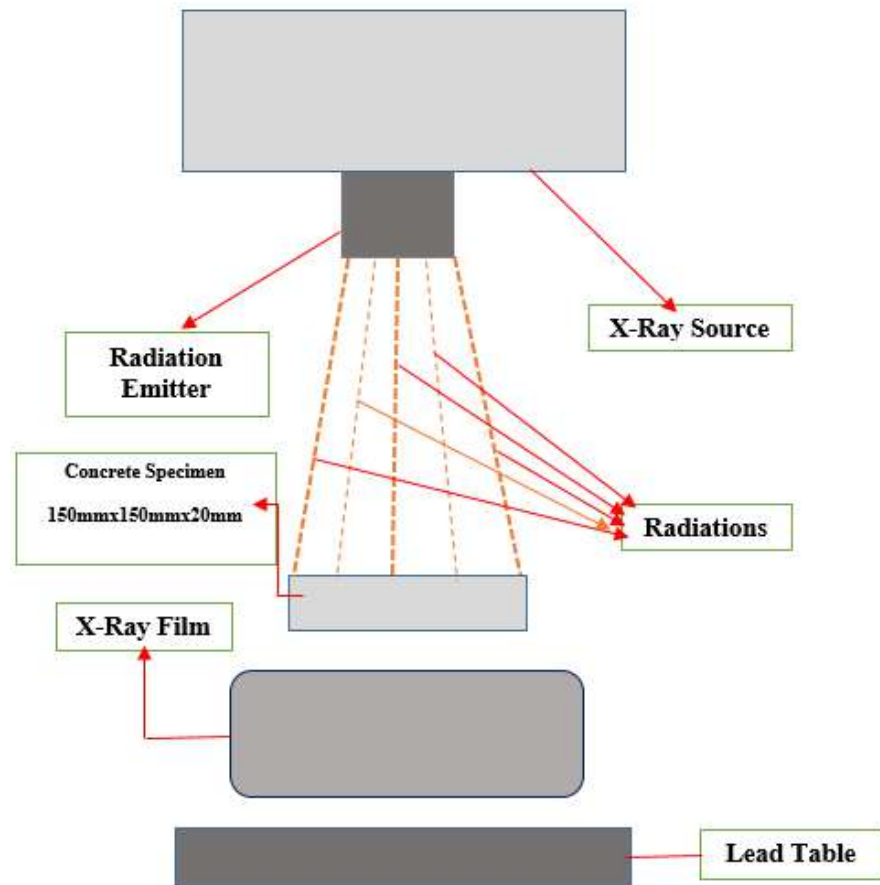


Figure 3-9 Experimental diagram of X-ray radiography

#### 2.3.4 Gamma Rays shielding test for micro studies of concrete specimens

The collimators alignment was achieved by using a laser pointer. To stop the built up ray to provide the lead collimators on both side of concrete samples. The specimens were placed in a vertical manner between the collimators. To stop any interference 3''x3'' NaI (TI) scintillation detector was appropriately shielded with lead cover to detect unobstructed gamma rays. With the help of NaI detector to recorded the gamma rays which was emitted by source which passed through collimators and penetrated as shown in figure 3.10.

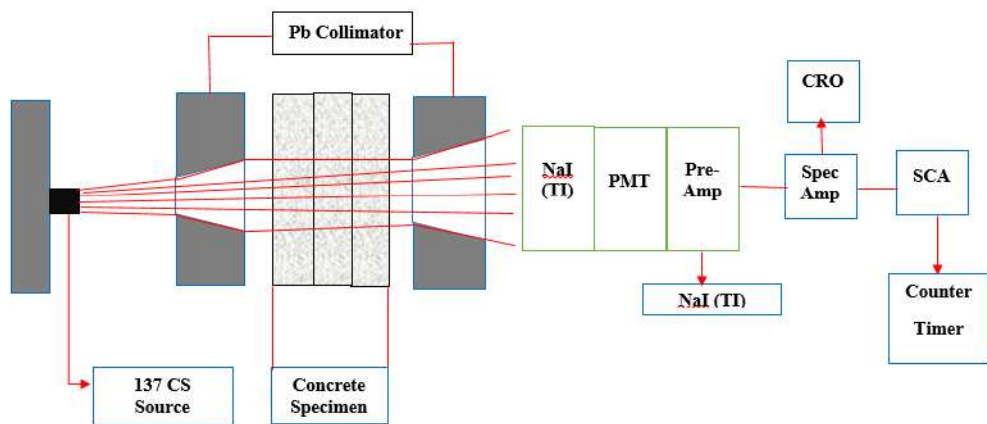


Figure 3-10 Experimental diagram of gamma rays attenuation

The distance between source point and detector was measured 380mm. For more information about the experimental setup can be found in details in given references [25]. For the weak detector signal must be needs to be amplified by the PMT before the shaped in the pre-amplifier. The impedance matched pre-amplifier which is further amplified in the spectroscopy amplifier. SCA choose a pulse of height that corresponds to the full energy peak, generating a digital pulse that is recorded by counter time. The accurate values of attenuation parameters were achieved by carefully choosing windows on the SCA a crucial factor in which obtains precise results. So, the experimental setup was calibrated by using Aluminum and Copper samples. The obtained results for the known samples exhibited strong agreement with previously published determining [39].

According to Lambert-Beer's Law its state that the transmission of radiation intensity through shields and number of quanta reaching the detector which applies to a narrow monochromatic beam of gamma rays.

Mathematically

$$I = I_0 e^{-\mu t} \#(1)$$

Here, I=Radiation Intensity after pass a certain thickness

$I_0$  = Without Sample Radiation Intensity  $t$  = Shield Thickness

And  $\mu$  = Linear Attenuation Coefficient of the sample

To eliminate the dependence on the physical state of the shielding material a new materials is called the mass attenuation coefficient is introduced. It is defined as the ratio of the linear attenuation coefficient to the density of material. in order to reduce reliance on the physical properties of the shielding material a novel term known as the mass attenuation coefficient has been introduced. This coefficient is defined as the ratio of the linear attenuation coefficient to the density of material.

Mathematically,

$$\mu_m = \frac{\mu}{\Delta} \quad \#(2)$$

Here,

Define in terms of Half-Value-Layer(HVL) , Tenth-Value-Layer(TVL) and also Mass coefficient ) as mathematically form

$$\frac{t1}{2} = \frac{\ln 2}{\mu} \quad (3)$$

### 2.3.5 Rebound Hammer Test on concrete specimens

It is Non-destructive test that can conduct on the concrete specimen. To determine the quality of concrete such as Excellence, Better Good, Fair and poor category. Rebound hammer depend on concrete hardness and surface that against mass strikes. According to standards specification ASTM 805 rebound hammer is shown in figure 3.11.





Figure 3-11 Rebound Hammer Test

Apply the force on the rebound hammer plunger which is pressed against the concrete surface and spring mechanism within the rebound hammer controls its action. The mass influenced by the hardness of concrete surface. The hardness of concrete and rebound values obtained from the graduated scale can be related with compressive strength of concrete. Noted the values and compared with standards range.

### **2.3.6 Ultra-Sonic Pulse Velocity on concrete specimens**

It is non-destructive test conducted on concrete specimens. To find out the quality of such Excellence, Better Good, Fair and poor.

Take a small amount of glycerin to put on surface of transmitter and receiver. In the procedure one transducer was placed in contact with surface of concrete and it moved along a predetermined path length within the concrete. Then, an electrical signal was transmitted to the second transducer, which was held against the opposite surface of the concrete element, and the measurement of the pulse time (T) was taken.

The pulse velocity find shown in equation 4. According to standards specification ASTM C597 ultra sonic pulse velocity shown the figure 3.12.

Mathematically

$$V = \frac{L}{T}$$

(4)

T=time

L=Length

V=velocity



Figure 3-12 Ultra-sonic Pulse Velocity Test

## CHAPTER-4

### 4. CALCULATIONS AND RESULTS

#### 4.1 Slump test:

To find average downward movement or determine the followability and check the workability of concrete. The maximum results was noted for HDC4 which is (76.2mm) and minimum was observed for HDC1 which is (48.8mm) all mixes values shown in blow table 4.1.

Table 4-1 Slump values

Mixes	Slump Values (mm)
CM	50.8
HDC1	48.26
HDC2	50.8
HDC3	63.5
HDC4	76.2



Figure 4-1 Slump test

#### 4.2 Concrete Density Fresh and Hardened

It was observed the maximum fresh density found for HDC4 which is 3438.44 (kg/m<sup>3</sup>) and minimum was found for CM which is 2102.31 (kg/m<sup>3</sup>) at room temperature.

Similarly the hardened density was maximum found HDC4 which is 3633.23 (kg/m<sup>3</sup>) at 100C → and minimum was noted for CM which is 2140.2 (kg/m<sup>3</sup>) at 300C → its show in table 4.2.

Mathematically:

$$\text{Density} = \text{Mass} / \text{Volume}$$

$$\text{Density} = M/V = 13\text{kg}/0.0035\text{m}^3 = 3633.23 \text{ (kg/m}^3\text{)}$$

Table 4-2 Densities of different concrete

Mixes	Fresh	28C→	100C→	200C→	300C→
CM	2102.32 (kg/m <sup>3</sup> )	2487.08 (kg/m <sup>3</sup> )	2250.12 (kg/m <sup>3</sup> )	2160.1 (kg/m <sup>3</sup> )	2140.23 (kg/m <sup>3</sup> )
HDC1	2645.4 (kg/m <sup>3</sup> )	2830.45 (kg/m <sup>3</sup> )	2730.23 (kg/m <sup>3</sup> )	2650.55(kg/m <sup>3</sup> )	2640.12 (kg/m <sup>3</sup> )
HDC2	3232.36 (kg/m <sup>3</sup> )	3440.34 (kg/m <sup>3</sup> )	3330.33 (kg/m <sup>3</sup> )	3250.46(kg/m <sup>3</sup> )	3255.32 (kg/m <sup>3</sup> )
HDC3	3379.16 (kg/m <sup>3</sup> )	3522.12 (kg/m <sup>3</sup> )	3400.23 (kg/m <sup>3</sup> )	3380.87(kg/m <sup>3</sup> )	3390.94 (kg/m <sup>3</sup> )
HDC4	3438.44 (kg/m <sup>3</sup> )	3633.23 (kg/m <sup>3</sup> )	3537.25 (kg/m <sup>3</sup> )	3469.49(kg/m <sup>3</sup> )	3460.32 (kg/m <sup>3</sup> )

### 4.3 Rebound hammer test

It is non-destructive test that can be conduct on concrete specimen. To find the quality of concrete such as Excellence, Better Good, Fair and poor category. The rebound hammer was maximum observed for HDC4 which is 36 and lies in the“ Good Layers” of concrete quality and minimum was found for CM which is 19.2 and lies in the “ poor Concrete category which is shown in table 4.3.

Taking average of rebound number minimum ten number required.

$$\text{Total Rebound No} = 21+17+17+18+23+20+20+21+17+18/ 10 = 19.2$$

Table 4-3 Rebound Hammer Test Results

Mixes	28C° (No)	100C° (No)	200C° (No)	300C° (No)
CM	19.2	23.8	24.4	28.2
HDC1	22.4	26.2	29	29.6
HDC2	31	30	31.2	32
HDC3	30	28.2	31	32
HDC4	33	34.3	33	36

### 4.4 Ultra-Sonic pulse Velocity

It is Nondestructive test that can be conduct on concrete specimens. The

purpose of this test to find the concrete quality such Excellence, Better Good, Fair and poor, concrete.

Mathematically

$$V = \frac{L}{T} \quad (5)$$

T=Time, L=Length and V=Velocity

The maximum UPV was found for CM which is (3898.06) m/sec at room temperature it lies in the range (3500-4500) show “Good” quality. The lowest UPV value was found for CM which is (2343.2) m/sec, at 300C → lies in the range (2000-3000) show “Poor” quality in table 4.4.

L=6 inch

Then apply velocity formula  $V=L/T$

$$UPV1=43$$

$$UPV2=45$$

$$UPV3=50$$

$$\text{Total UPV} = 43+45+50/3=46$$

Convert micro sec to Sec then multiply  $10^{-6}$

$$\text{Time} = 46*10^{-6}=0.000046 \text{ sec}$$

$$\text{Then } L= 0.1524\text{m}$$

$$V = L/T = 0.1524/0.000046=3313.98\text{m/sec}$$

Table 4-4 Ultra-Sonic pulse Velocity Test Results (m/s)

Mixes	28C →	100C°	200C°	300C°
CM	2998.8 (m/sec)	2889.4 (m/sec)	2678.3 (m/sec)	2343.2 (m/sec)
HDC1	3313.98(m/sec)	3350.3 (m/sec)	3286.5 (m/sec)	3013.2 (m/sec)
HDC2	3460.4 (m/sec)	3358.7 (m/sec)	3310.9 (m/sec)	3232.4 (m/sec)
HDC3	3697.7 (m/sec)	3563.5 (m/sec)	3433.6 (m/sec)	3333.5 (m/sec)
HDC4	3898.6 (m/sec)	3811.4 (m/sec)	3733.32(m/sec)	3670.7 (m/sec)

## 4.5 Compressive Strength Test

The highest compressive strength value was found for HDC3 which is 35.05 MPa at 300C $\rightarrow$ . The lowest compressive strength value was observed for CM 12.35 MPa at 100C $^{\circ}$  in table 4.5.

Specimen, compression load

Maximum stress= P/A

Area 150mm x 150mm x150mm

Table 4-5 Compressive Strength (MPa)

Mixes	28C $\rightarrow$		100C $^{\circ}$	200C $^{\circ}$	300C $^{\circ}$
CM	27.55 (MPa)		12.38 (MPa)	19.48 (MPa)	22.69 (MPa)
HDC1	25.79 (MPa)		15.1 (MPa)	16.44 (MPa)	18.39 (MPa)
HDC2	29.58 (MPa)		24.69 (MPa)	17.84 (MPa)	23.72 (MPa)
HDC3	34.63 (MPa)		16.03 (MPa)	26.95 (MPa)	35.05 (MPa)
HDC4	30.34 (MPa)		33.15 (MPa)	24.05 (MPa)	29.23 (MPa)

## 4.5 Concrete X rays test

For the study and analysis of the internal structure and core of the concrete specimens to perform the X-ray radiography test. X-ray test perform on HDC3, HDC4 and CM at different temperature.

HDC4, at 200C $\rightarrow$ , HDC2 at room temperature have shown large amount of voids, cracks, which show that weak bond between aggregates and cement paste.

On the other side the HDC3 at 300C $\rightarrow$  is show minimum voids that why it show maximum compressive strength because due to strong bond between aggregates and cement paste.

## 4.6 Scanning electron Microscope (SEM) testing

To study and analysis of the microstructure and topography of the concrete specimens. For this purpose of study to performed scanning electron microscope testing (SEM). Taken the image at different magnification at 5000X (5 $\mu$ m) and 10000X (1 $\mu$ m).

CM at 100C $\rightarrow$  show large amount of pores, maximum voids, bond cracks and less amount of C-S-H gel that why it loss compressive strength.

Similarly HDC3 at 300C $\rightarrow$  show large amount of C-S-H gel, minimum voids, minor cracks and low porosity that why its show maximum compressive strength.

## 4.7 Linear attenuation coefficient

The linear attenuation coefficient of the heavy density concrete (HDC) is shown in Fig 10(d).The maximum values was noted for HDC4 at 300C $\rightarrow$  which is 0.249cm<sup>-1</sup> and minimum was 0.17cm<sup>-1</sup> for CM at room temperature. Where others mixes at different elevated temperature highest value was found HDC1 which is 0.225cm<sup>-1</sup> at 200C $\rightarrow$ , HDC2 which is 0.222cm<sup>-1</sup> at 100C $\rightarrow$  and HDC3 which is 0.183cm<sup>-1</sup> at 100C. and lowest values was observed at different elevated temperature for HDC1 which is 0.18cm<sup>-1</sup> at 28C, HDC2 which is 0.182cm<sup>-1</sup> at 200C $\rightarrow$  and HDC3 which is 0.19cm<sup>-1</sup> at 300C $\rightarrow$ .

## 4.8 Mass attenuation coefficient

The mass attenuation coefficient of heavy density concrete (HDC) show in Fig 10(e). The highest value was noted for HDC4 0.063 cm<sup>2</sup>/g and lowest was found HDC1 which is 0.0848 cm<sup>2</sup>/g at 200C $\rightarrow$ . The result is show that by the increasing of Heavyweight aggregates Grit Iron Scale Aggregates (GISA) increasing the attenuation coefficient. The attenuation coefficient of HDC4 mixes show decreased with temperature at room temperature which is 0.063cm<sup>2</sup>/g and 100C $\rightarrow$  0.065cm<sup>2</sup>/g.

## **4.9 Half Value Layer, Tenth Value Layer and Mean**

### **Free Path**

The half value layer highest was found for CM mix which is 4.78cm at 100C→ and lowest was found for HDC4 which is 3.01cm at 100C→ shown Fig 5.11(a). The Tenth value layer maximum was noted for CM which 15.87cm at 100C→ and minimum was noted HDC4 which is 9.24 at 28C→ and 300C→ shown in fig 5.11(b).the maximum mean free path was measured for CM which is 6.89cm and minimum was measured for HDC4 which is 4.01cm at 28C→ and 300C→ show in fig 5.11(c). All the results of HVL and TVL and mean free path shown in table 5.2.



## CHAPTER-5

### 5. ANALYSIS OF RESULTS

#### 5.1 Workability and Slump

The workability of concrete tends to increase by increasing the content of HWGS. The lowest slump was observed for mix HDC1, which contains 25% HWGS aggregates due to large surface area of MgO and binding effect on water which reduced the followability of concrete. In the modified mixes, HDC1 and HDC2 demonstrated the greatest workability and fit the ACI Mix Design's specification range. The four factors maximum size of coarse aggregate, gradation of particles, surface texture, and shape of the aggregates could be assessed in order to best explain the workability of concrete [40]. But the density also include with heavyweight aggregates. During mixing, the heavyweight aggregates attempt to settle down, which causes bleeding and segregation. HWGS aggregates shape are angular and rough-textured.

Therefore, the slump of concrete increase when increasing the content of HWGS aggregates [41]. Then make mechanical interlocking due to angular shape and rough texture of the HWGS aggregates. To make the paste workable and reduce intra-particle friction, more efforts is required [42]. The slump value for the control mix was found to be 50.8 mm whereas HDC1, HDC2, HDC3, and HDC4 showed Slump of 48.26 mm, 50.8 mm, 63.5 mm, and 76.2 mm respectively. Smaller aggregates were added, which may be the cause of the CM mix slump decreasing incorporated (5 – 9mm). The smaller aggregates can move easy with other particles, creating a ball-bearing effect in a mix. A slump is decreased when the size of the coarse aggregate is increased. Figure 5.1 illustrates a slump's fluctuation.

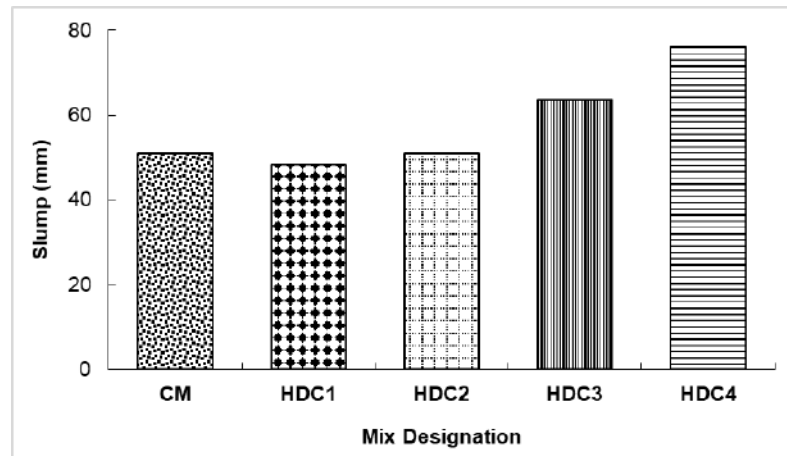


Figure 5-1 Slump and Mix Designation

## 5.2 Loss of mass and density

The change in mass and density on elevated temperature graphical results as shown in Figures 5.2 (a) and 5.2(b). It was noted that the linear increased in mass and density with elevated temperatures. The concrete properties to be affected the composition of aggregates and size. However, Grit Iron Scale Aggregates concrete down relative loss as compared to controlled mixes. Figures 5.2(a) and 5.2(b) the results is show that mass and density loss with elevated temperature. It was noted maximum density loss for HDC4 which is 3.12% at 300C $\rightarrow$  and minimum density loss 0.55% for HDC2 at 100C $\rightarrow$ .

The variation between 200C $\rightarrow$  to 300C $\rightarrow$  are because due to physical changes and breakdown occur inside the cement matrix. All free bound and unbound water tends to evaporate at high temperature [43].

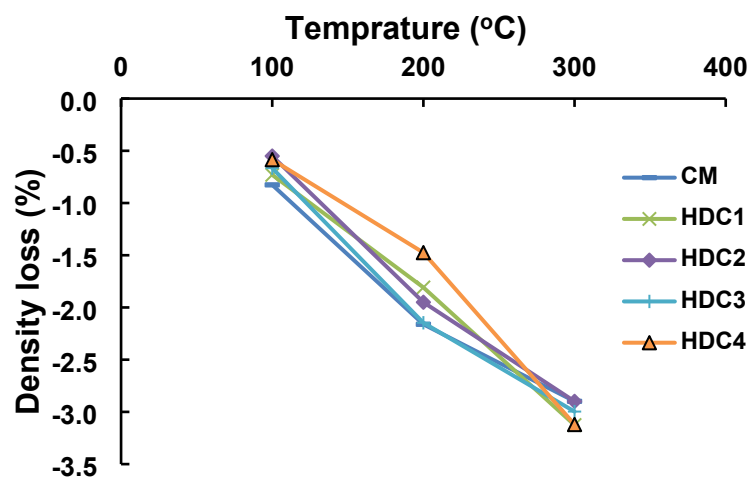


Figure 5-2(a) Relative density loss against temperature

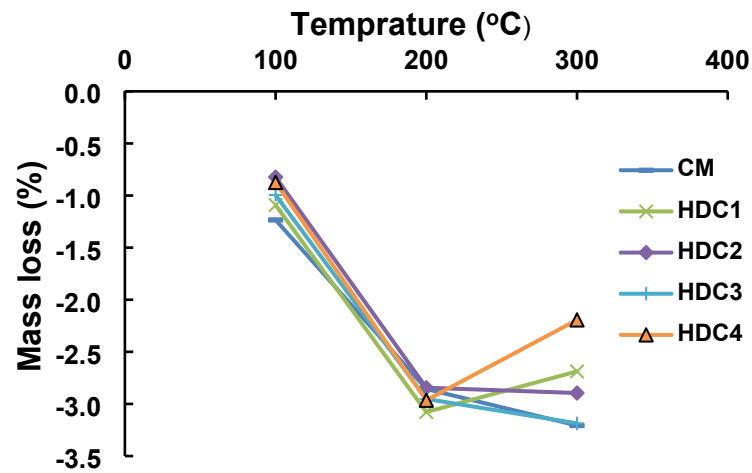


Figure 5-3(b) Relative mass loss against temperature

### 5.3 Densities

The density of different concrete mixes with different temperature such as (28C→,100C→,200C→ and 300C→). At room temperature the maximum fresh density was found for HDC4 which was found to be 3438.44 (kg/m<sup>3</sup>) and lowest was observed for CM at room temperature which was found to be 2102.31 (kg/m<sup>3</sup>).

The largest hardened density was observed for HDC4 which was found 3633.23 (kg/m<sup>3</sup>) at 100C→ and lowest was observed for CM which was noted 2140.2 (kg/m<sup>3</sup>) at 300C→.

The densities results is show that the hardened density is more than fresh density. Due to because the present of air voids and water in the fresh mixes. And also lesser specific gravity.

The hardened density is show more than fresh density. Due to all bound and unbound water evaporates the cement particles react with chemically with water to make strong bond of hydration [25]. Figure 5.4

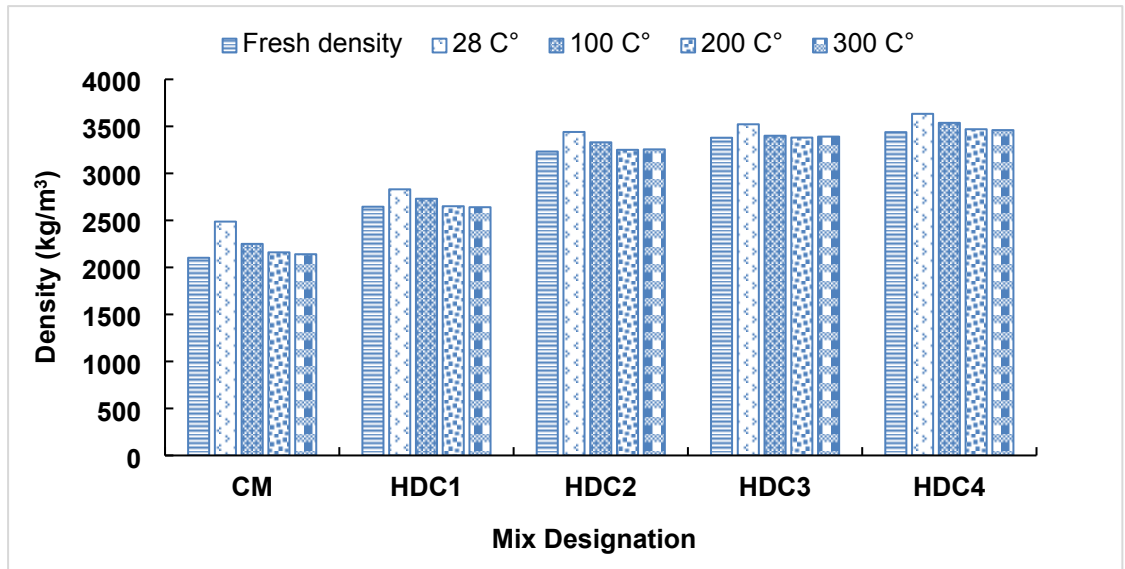


Figure 5-4 Fresh and hardened density variation with mix designation

## 5.4 Rebound Hammer Test

Rebound hammer results show that the maximum values were observed in HDC4 having 100% HWGS aggregates, which was found to be 36 and lies in the “Good Layers” of the concrete quality. The lowest was noted for CM, which was found to be 19.2 and lies in the “poor Concrete” category. Shown in the figure 5.5

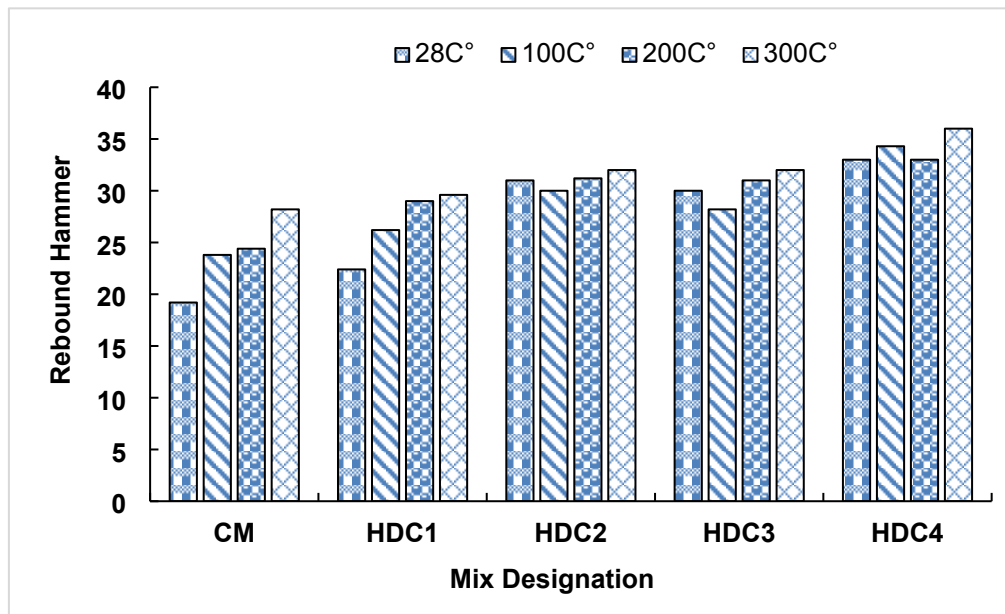


Figure 5-5 Rebound Hammer variation with mix designation

## 5.5 Ultra-sonic Pulse Velocity Test

The ultrasonic pulse velocity results is show that the largest values was obtained HDC4 which was found to be 3898.6m/sec at room temperature its lies good quality of concrete. The lowest was found for CM which was found to be 2343.2m/sec at 300C → its lies poor quality of concrete. Due to the grit scale aggregates are made or composed of heavy and dense structures with high atomic weight [41]. So the pulses of UPV are easily attenuated by the dense atomic structure of the concrete to because the inclusion of grit scale aggregates hence resulting in more value shown in figure 5.5.

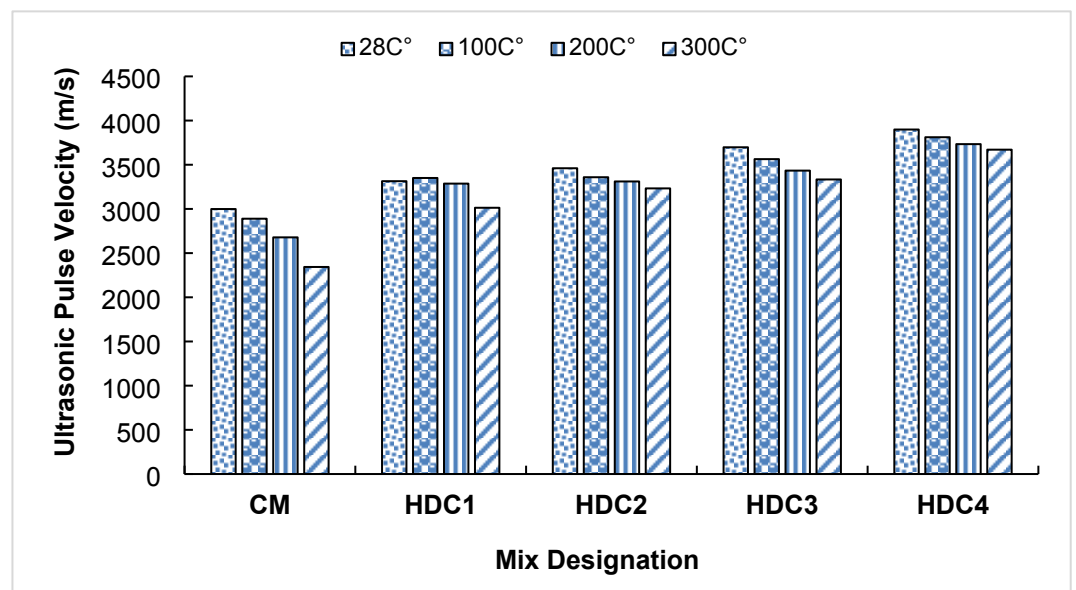


Figure 5-6 Ultra-sonic Pulse Velocity variation with mix designation

## 5.6 Compressive strength

There are different phase of compressive strength increased or decreased to because the temperature variation in the range of 28C → to 300C → as shown in figure 5.7. The temperature between 28C → to 100C → are show minor change in the concrete specimens. The temperature between 100C → to 200C → to increase as compare to 28C → to 100C → but less than to 300C →. It was observed that the maximum compressive strength the variation of temperature

at the range of 200C $\rightarrow$  to 300C $\rightarrow$ . the same pattern was observed and finding our report by Thomas et al, and Sheriff et al, [44], [44].

HDC2, HDC3 and HDC4 concrete mixes strength at 200C $\rightarrow$  and 300C $\rightarrow$  results show increased from 28C $\rightarrow$ . the changing of concrete compressive strength increases or decreases due the main reason only the anhydrous cement particles chemical reaction that occur because of heating .the anhydrous cement particles individual base found in the calcium silicate usually consist of multiple fragments and also presences of various crystalline phases like C3S, C3S and other minor particles the same was investigated by Horszczqruk et al. and Hager [45],[46].

The anhydrous cement particles are present in all concrete with finer particles having tendency to hydrate more rapidly. During the heating anhydrous cement particles change phase into anhydrous cement component with improving or enhancing the compressive strength.

The maximum compressive was observed HDC3 (35.05 MPa at 300C $\rightarrow$ ) and minimum was observed in CM (12.5 MPa at 100C $\rightarrow$ ). The result is show that up to 75% replacement of NCA with GISA tend to increase the compressive strength of concrete. Because of grit iron scale aggregates tend to make strong bond due to angular and irregular structure of aggregates[25].

Fig 5.7 show compressive strength

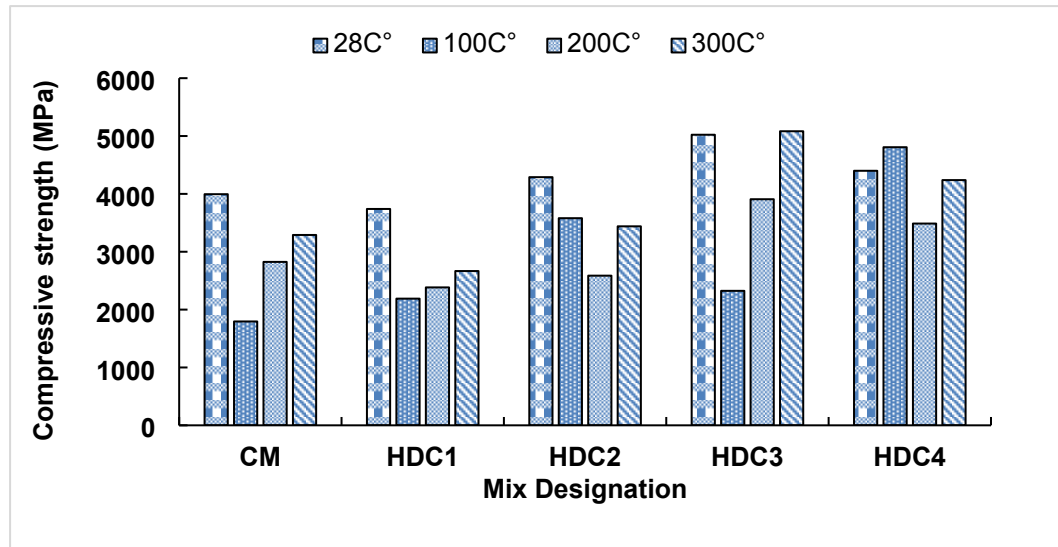


Figure 5-7 Compressive strength of specimen at various temperatures

## 5.7 X-Ray radiography core of concrete specimens

For the study and analysis of the internal structure and core of the concrete specimens to perform the X-ray radiography test. The contrasting core structure of HDC3 concrete sample at ambient temperature 300C is shown in Fig 5.8(a) and 5.8(b). The X-rays radiography result of HDC3 show that the compact dense structure with dark shades and a few voids at room temperature observed that a strong solid bond between aggregates and cement paste. Therefore, due to because of high heating inside the concrete specimens. So, it can be seen easily in mix HDC3 having minimum voids, dark shed it show that strong bond between aggregates and cement paste. That why the HDC3 show maximum compressive strength at 300C→.

On the other hand the specimens of CM, HDC4, at 200C→, HDC2 at room temperature having seen large amount of cracks present in the specimens which show that badly degraded of the specimens. So, maximum voids, large cracks to indicated the lesser bond between aggregates and cement paste.

The specimens of controlled mixes (CM) having present maximum number of voids and gas pocket which show that reduced the compressive strength. The

internal structure of the specimens having full of gas pockets because of the phase change at elevated temperature.

HDC4, at 200C→, HDC2 at room temperature have maximum amount of voids and cracks in internal side which indicate weak bond between aggregate and cement paste. That why it loss the compressive strength. On the other side the HDC3 at 300C→ is show minimum voids, cracks that why it show maximum compressive strength because due to strong bond between aggregates and cement paste[25].

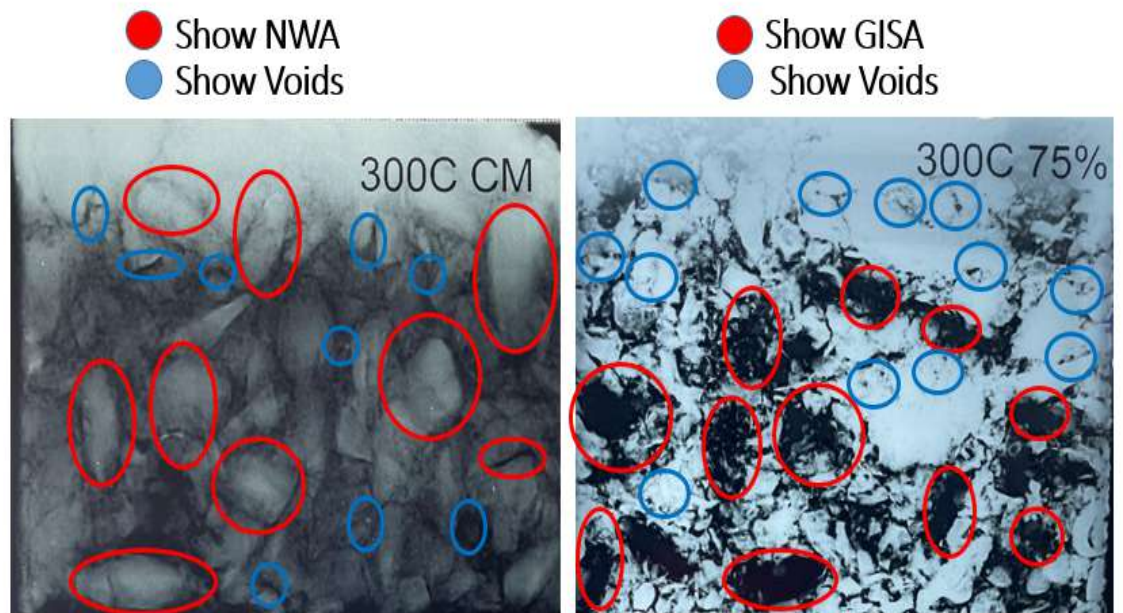


Figure 5-8(a) X-Ray simple (CM 300C→, 75% 300C→)



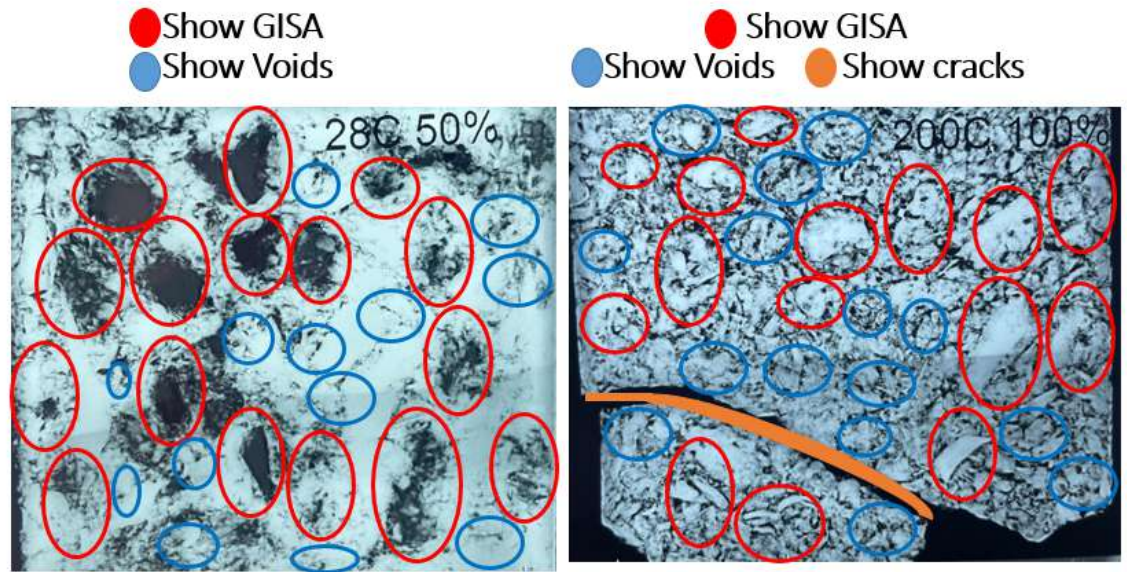


Figure 5-8 (b) X-Ray simple (28C → 50%, 200C → 100%)

## 5.8 Scanning electron Microscope (SEM) testing

To study and analysis of the microstructure and topography of the concrete specimens. For this purpose of study to performed scanning electron microscope testing (SEM). Taken the image at different magnification at 5000X (5 $\mu$ m) and 10000X (1 $\mu$ m).

The magnification at 5  $\mu$ m image were utilized to examine the overall structure characteristic of the cement paste including cracks, gaps and interfaces under various heating temperature. Meanwhile the 1  $\mu$ m image were employed to study mineral phase transformation the emergency of new product and mineral recrystallization across at different heading temperature show in Fig. 5.9(a) and 5.9(b). The C-S-H gel show direct relation with compressive strength and porosity or voids show inversely relation with them.

The results is show that a large amount of C-S-H gel can be seen in HDC3 at 300C → specimens of concrete and porosity was observed low that why HDC3 show maximum compressive strength. On the other hand more voids large micro cracks can be seen in the CM mixes at 100C → due to more porosity and

less amount of C-S-H gel was found lack of cohesion in the paste due to reverse hydration [25]. Fig. 5.9(a) and 5.9(b).

### Controlled mixes (CM) at 100C°

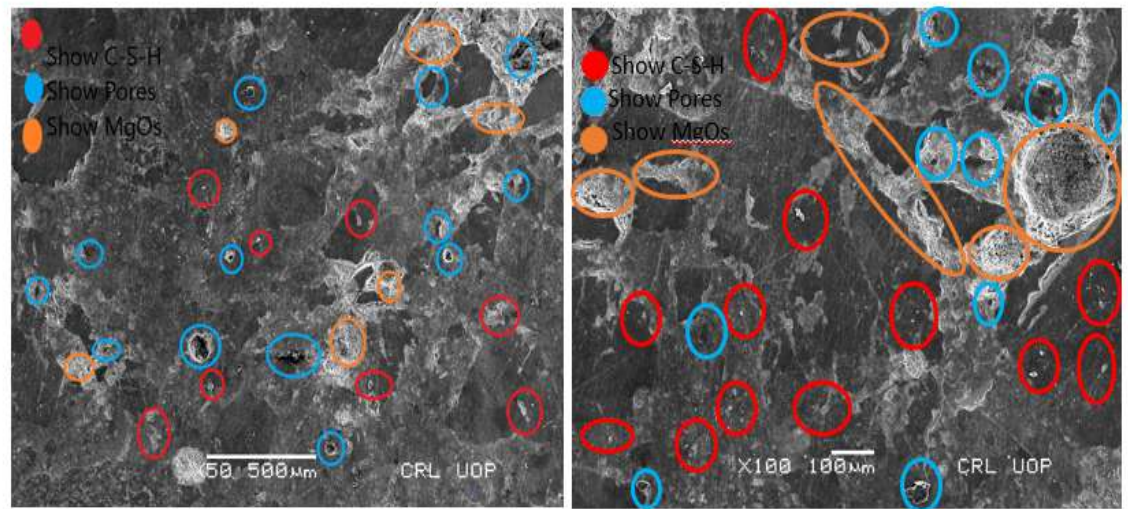


Figure 5-9(a) Show SEM Analysis at (CM 100C→)

### HDC3 at 300C°

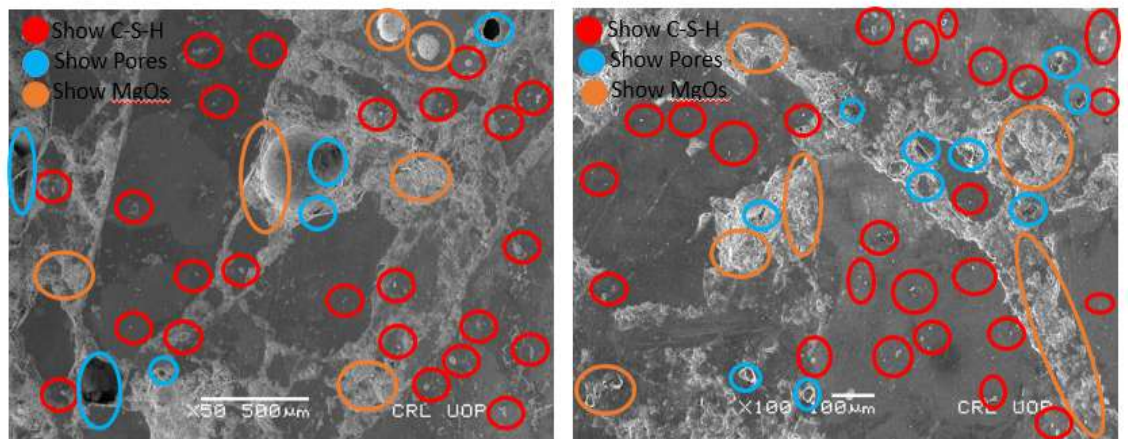


Figure 5-9 (b) Show SEM Analysis at (HDC3 300C→)

## 5.9 Gamma ray attenuation coefficient

With the help of slope of intensity thickness graph were determined linear attenuation and mass attenuation coefficient show in fig 5.10 (a) and 5.10(b).HDC1 mixes at 300C $\rightarrow$  was observed 0.225 cm<sup>-1</sup>. Table 5.1 are show the values of mass and linear attenuation with relation of different temperature and mixes. The attenuation coefficient maximum values was found HDC4 at room temperature which is 0.249cm<sup>-1</sup> at 300C and minimum CM 0.17cm<sup>-1</sup> at room temperature show in 5.10 (b) and(c). The CM mixes the linear attenuation coefficient tends to increase with increased temperature up to 300C $\rightarrow$ . At 100C $\rightarrow$ -200C $\rightarrow$  the linear attenuation coefficient of HDC3 maximum decreased from 0.183cm<sup>-1</sup> to 0.21cm<sup>-1</sup>.similarly linear attenuation coefficient of HDC4 down 0.229cm<sup>-1</sup> to 0.23cm<sup>-1</sup> at 28C $\rightarrow$  -100C $\rightarrow$  and at the range of 200C $\rightarrow$ -300C $\rightarrow$  CM, and HDC1 show decreased linear attenuation coefficient. HDC2, HDC3, and HDC4 show increased. The same results is show nearly values in the range of 28C $\rightarrow$  to 300C $\rightarrow$  of linear attenuation coefficient in Fig 10(d). Mass attenuation coefficient with same trend determines with different temperature is show in the Fig 10(e).The above decreased due all free and bound unbound water evaporated at 100C $\rightarrow$ , 200C $\rightarrow$  and 300C $\rightarrow$ . The temperature range 200C $\rightarrow$  to 300C $\rightarrow$  show minor change on the concrete physical properties there is minor loss due to chemically bound water evaporate. The decreased trend of mass attenuation up to 300C $\rightarrow$  because the main reason is dehydration of C-S-H gel and loss of chemically bound water show in Fig 10 (d) [25].

Table 5.1 Linear and mass attenuation coefficient with differen mixes and differen temperature

28C $\rightarrow$	100C $\rightarrow$	200C $\rightarrow$	300C $\rightarrow$

Name of Mixes	$\mu(c m^{-1})$	$\mu_{\text{eff}} \Delta(c m^2/g)$	$\mu(c m^{-1})$	$\mu_{\text{eff}} \Delta(c m^2/g)$	$\mu(c m^{-1})$	$\mu_{\text{eff}} \Delta(c m^2/g)$	$\mu(c m^{-1})$	$\mu_{\text{eff}} \Delta(c m^2/g)$
CM	0.17	0.068	0.145	0.0644	0.174	0.0805	0.159	0.0742
HDC1	0.18	0.0635	0.169	0.0618	0.225	0.0848	0.195	0.0738
HDC2	0.213	0.0619	0.222	0.0666	0.182	0.0559	0.187	0.0574
HDC3	0.177	0.0503	0.183	0.0538	0.21	0.0621	0.19	0.056
HDC4	0.229	0.063	0.23	0.065	0.226	0.0651	0.249	0.0719

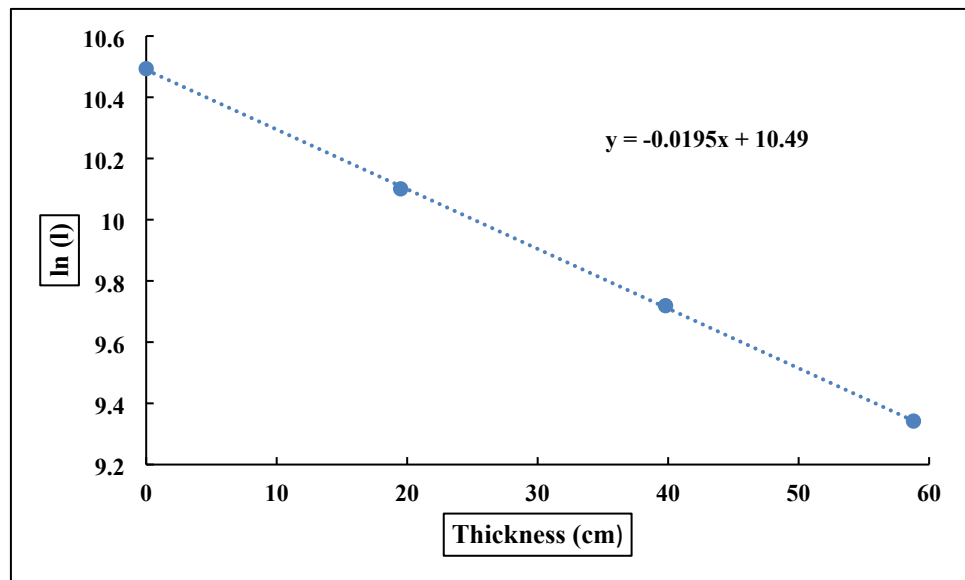


Figure 5.10 (a) linear attenuation coefficient concrete specimen at 300C →

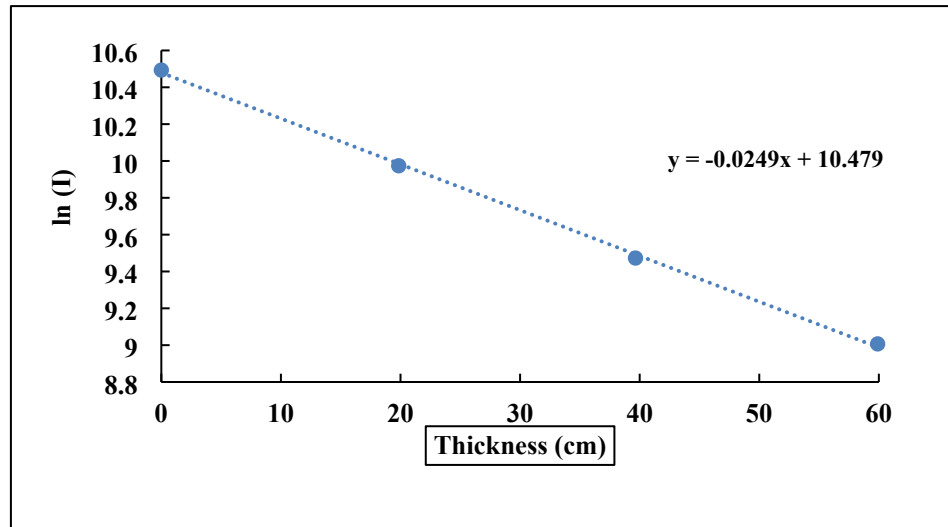


Figure 5.10(b) linear attenuation coefficient HDC4 at 300C →

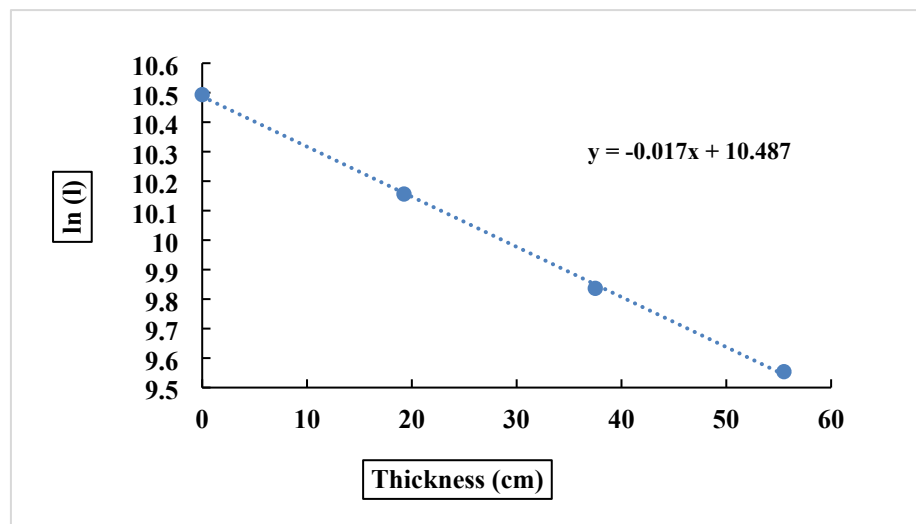


Figure 5.10 (c) linear attenuation coefficient CM at room temperature

## 5.10 Linear attenuation coefficient

The linear attenuation coefficient of the heavy density concrete (HDC) is shown in Fig 10(d). The maximum values was noted for HDC4 at 300C → which is 0.249cm<sup>-1</sup> and minimum was 0.17cm<sup>-1</sup> for CM at room temperature. Where others mixes at different elevated temperature highest value was found HDC1 which is 0.225cm<sup>-1</sup> at 200C →, HDC2 which is 0.222cm<sup>-1</sup> at 100C → and HDC3 which is 0.183cm<sup>-1</sup> at 100C. and lowest values was observed at different elevated temperature for HDC1 which is 0.18cm<sup>-1</sup> at 28C, HDC2 which is 0.182cm<sup>-1</sup> at 200C → and HDC3 which is 0.19cm<sup>-1</sup> at 300C →. The linear

attenuation coefficient decreased due to all free and bound unbound water evaporated at 100C $\rightarrow$ , 200C $\rightarrow$  and 300C $\rightarrow$ . The temperature range 200C $\rightarrow$  to 300C $\rightarrow$  show minor change on the concrete physical properties there is minor loss due to chemically bound water evaporate. The decreased trend of mass attenuation up to 300C $\rightarrow$  because the main reason is dehydration of C-S-H gel and loss of chemically bound water show in Fig 10 (d)[25].

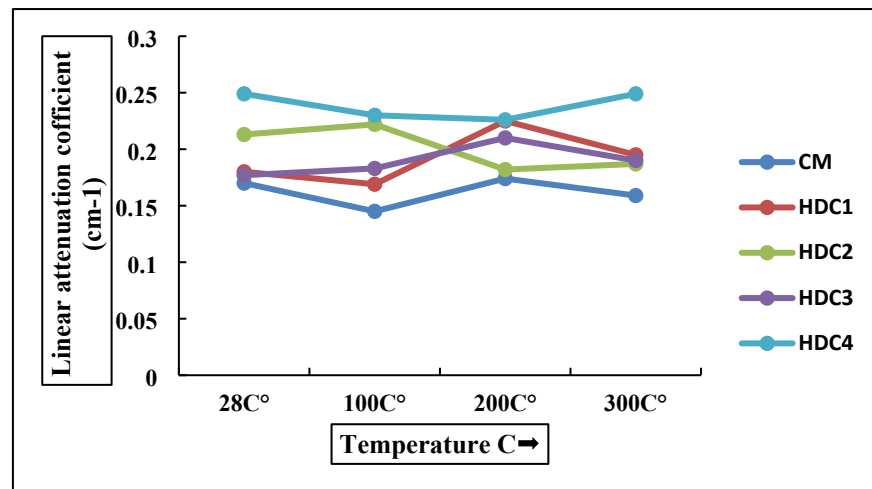


Figure 10 (d) linear attenuation coefficient of HDC concrete with temperature

### 5.11 Mass attenuation coefficient

The mass attenuation coefficient of heavy density concrete (HDC) show in Fig 10(e). The highest value was noted for HDC4 0.063 cm<sup>2</sup>/g and lowest was found HDC1 which is 0.0848 cm<sup>2</sup>/g at 200C $\rightarrow$ . The result is show that by the increasing of Heavyweight aggregates Grit Iron Scale Aggregates (GISA) increasing the attenuation coefficient. The attenuation coefficient of HDC4 mixes show decreased with temperature at room temperature which is 0.063cm<sup>2</sup>/g and 100C $\rightarrow$  0.065cm<sup>2</sup>/g. HDC4 concrete show good quality of mechanical properties the concrete is most important for attenuation. The decreased and increased may be due to hydration of unhydrated C-S-H between 100C $\rightarrow$  to 300C $\rightarrow$ . The lowest attenuation was noted for HDC1 concrete at 200C. This is show decreased mass attenuation because of degradation of matrix and cracks inside the concrete. With elevated temperature all free bound and unbound water evaporate in the cement matrix which lead to high penetration power of gamma rays.



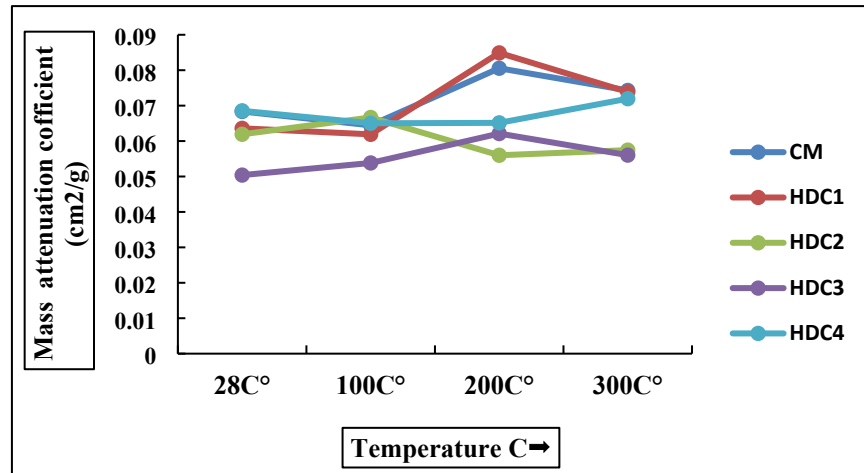


Figure 10(e) Mass attenuation coefficient with different temperature

## 5.12 Half Value Layer, Tenth Value Layer and Mean Free Path

The half value layer highest was found for CM mix which is 4.78cm at 100C→ and lowest was found for HDC4 which is 3.01cm at 100C→ shown Fig 5.11(a). The Tenth value layer maximum was noted for CM which 15.87cm at 100C→ and minimum was noted HDC4 which is 9.24 at 28C→ and 300C→ shown in fig 5.11(b).the maximum mean free path was measured for CM which is 6.89cm and minimum was measured for HDC4 which is 4.01cm at 28C→ and 300C→ show in fig 5.11(c). All the results of HVL and TVL and mean free path shown in table 5.2.

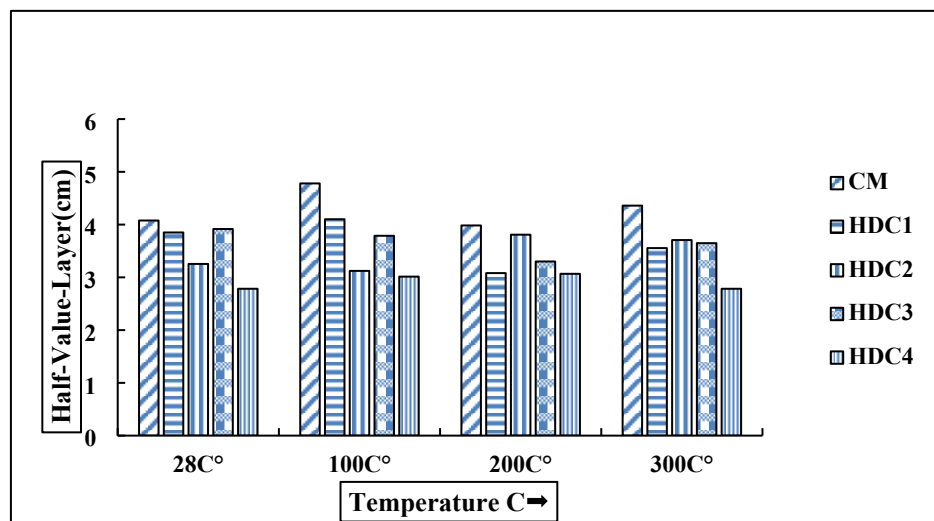


Figure 5.11(a) Half Value Layer us Temperature

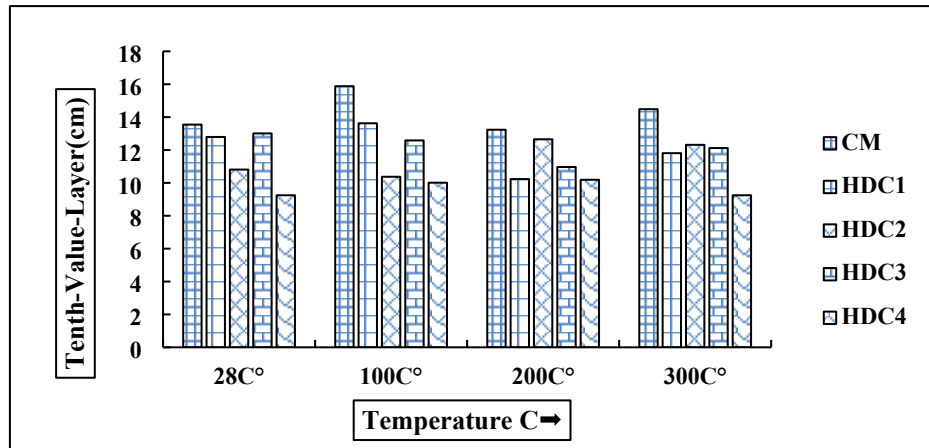


Figure 5.11(b) Tenth Value Layer us Temperature

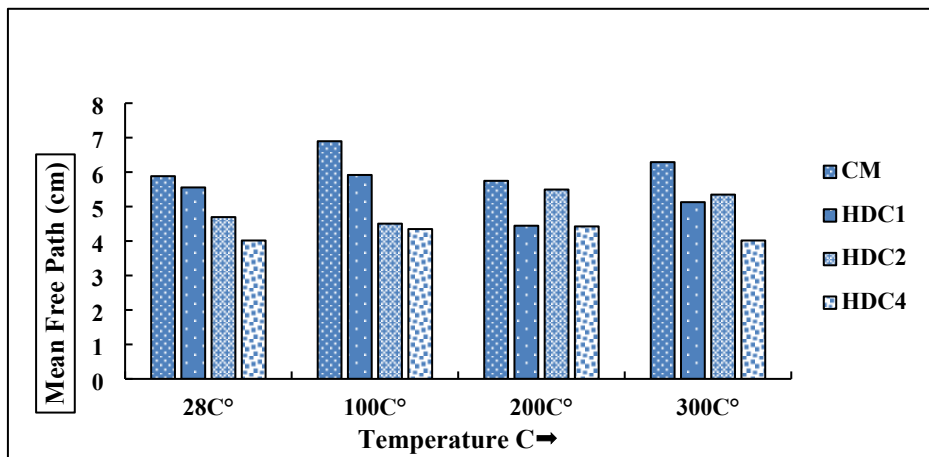


Figure 5.11(c) Mean Free Path us Temperature

Table 5.2 Show results of HVL, TVL and Mean free Path at different temperature

Temperature	CM			HDC1			HDC2			HDC3			HDC4		
	HVL(cm)	TVL(cm)	Mean Path(cm)	HVL(cm)	TVL(cm)	Mean Path(cm)	HVL(cm)	TVL(cm)	Mean Path(cm)	HVL (cm)	TVL (cm)	Mean Path(cm)	HVL(cm)	TVL(cm)	Mean Path(cm)
28°C	4.07	13.54	5.88	3.85	12.79	5.55	3.25	10.81	4.69	3.91	13	5.64	2.78	9.24	4.01
100°C	4.78	15.87	6.89	4.1	13.62	5.91	3.12	10.37	4.5	3.78	12.58	5.46	3.01	10.01	4.34
200°C	3.98	13.23	5.74	3.08	10.23	4.44	3.8	12.65	5.49	3.3	10.96	4.76	3.06	10.18	4.42
300°C	4.35	14.48	6.28	3.55	11.8	5.12	3.7	12.31	5.34	3.64	12.11	5.26	2.78	9.24	4.01



## CHAPTER-6

### 6. BUDGETING AND COSTING OF THE PROJECT

The cost of normal weight concrete is compared with that of heavy density concrete. The cost of cement in PKR =1050, where the Sand and normal coarse aggregates costs about PKR= 250 kg (as per December 2022 statistics).

The cost of MgO in PKR =300 kg (as per December 2022 statistics). Heavy weight aggregates Grit iron Scale aggregates sponsored from the side Dr.Nasir Ayaz Khan.

Then successfully used of MgO as a 5 % replacement for cement could further improve the compressive strength, Rebound hammer, Ultra-sonic Pulse Velocity.

The volume of cube

#### 6.1 Cost per m<sup>3</sup> of heavy density concrete

Table 6-1 Cube volume

Volume of cube	6"X6"X6"	0.0035 m <sup>3</sup>
Total Volume of cube	40× 0.0035	0.14 m <sup>3</sup>

The total casted of cubes

Table 6-2 Quantity of material

Mixes	Room Temperature	100C→	200 C→	300 C→
CM	2	2	2	2
HDC1	2	2	2	2
HDC2	2	2	2	2
HDC3	2	2	2	2
HDC4	2	2	2	2

Total	10	10	10	10
-------	----	----	----	----

Totally 40 cubes were casted

$$V = 0.150 \times 0.150 \times 0.15$$

Cost of cement, sand and coarse aggregates

Table 6-3 Material costs

Materials	Cost (Rs)
Cement	2000
Sand	1500
Normal Coarse Aggregates	3000
Grit iron scale Aggregates	0
MgO	300
Total	6800

=total cost / total Volume of cubes

$$\text{PKR} = 6800 / 0.14 = 48572 \text{ PKR/m}^3$$

Costs Testing and Cutting

Table 6-4 Testing expenses

Name of testing	Cost (Rs)
Cutting of Cubes	4000
X-Ray Testing	700
SEM Testing	11000
Gamma Rays Testing	5000

For normal weight concrete the Cost of cement, sand and coarse aggregates

Table 6-5 Normal weight concrete costs

Materials	Cost (Rs)
-----------	-----------

Cement	2100
Sand	1500
Normal Coarse Aggregates	4500
Total	8100

=total cost / total Volume of cubes

$$\text{PKR} = 8100 / 0.14 = 57857 \text{ PKR/m}^3$$

This heavy density concrete is still less expensive normal weight concrete because the grit iron scale is waste and will be freely available while in case of normal weight concrete the aggregated cost need to count.

## CHAPTER-7

### 7. CONCLUSION

The slump of concrete is increased when we increased the grit iron scale aggregates. The highest was observed for HCD4 and lowest was measured for HDC1. The MgO particles binding effect and surface area which reduced the followability and workability of concrete that why HDC1 show lowest slump. In the fresh density contain some air voids and water. Other hand hardened density all bound and unbound water tends to evaporate therefore, the hardened density was observed more than fresh density. Non-destructive test rebound hammer maximum was noted for HDC4 which is 36 its show “Good quality of concrete” and minimum was noted for CM which is 19.2 its show “poor quality of concrete”. Second non-destructive test Ultra-sonic pulse velocity largest was noted for HDC4 at room temperature which was (3898.06) m/sec it lies in the range (3500-4500) show “Good” quality. Minimum UPV value was found for CM (2343.2) m/sec, at 300C → lies in the range (2000-3000) show “Poor” quality. Maximum density loss of 3.12% for HDC4 at 300 °C and minimum density loss 0.55% for HDC2 at 100 °C. Maximum value of compressive strength was found for HDC3 (35.05) MPa at 300 °C and minimum value of 12.35 MPa obtained for CM at 100 °C. X-ray radiography is show best result for HDC3 at 300°C and poor results for CM at 300°C. SEM is show best results for HDC3 at 300°C and poor result for CM at 100°C.

The linear attenuation coefficient maximum values was noted for HDC4 at 300C which is 0.249cm<sup>-1</sup> and minimum was 0.17cm<sup>-1</sup> for CM at room temperature. Mass attenuation coefficient highest value was noted for HDC4 0.063 cm<sup>2</sup>/g and lowest was found HDC1 which is 0.0848 cm<sup>2</sup>/g at 200C →.

Therefore the results is show that heavy density concrete made by Grit Iron Scale Aggregates show more efficient in attenuating gamma rays at all

temperature. It is depend upon density which improve HVL values. The minimum was noted for controlled mix CM. The attenuation of CM was very weak and unable to be used for measurements.

## **CHAPTER-8**

### **8. RECOMMENDATIONS AND FUTURE PROSPECTS**

In the given study, the normal weight aggregate is replaced with 25, 50, 75 and 100% replacement. This study can be further extend in of the following ways.

- ◆ To study the properties of Grit Iron Scale heavy density concrete with 5 % MgO's at elevated temperature of 400C→, 500C→, upto 1200C→ and may improve the strength.
- ◆ To used high density aggregates for concrete composition like Barite, Magnetite to improve attenuation power and observed harmful gamma radiation make it suitable for nuclear power plants, medical facilities, and archeological site and research laboratories.
- ◆ To enhanced the structure strength by adding heavy weight aggregates
- ◆ Heavyweight concrete with grit iron scale aggregates may result in more sustainable and eco-friendly environment materials. By incorporating recycled or waste as grit iron scale aggregates, like crushed industrial by- products.

## BIBLIOGRAPHY (IEEE REFERENCE STYLE SHOULD BE ADOPTED):

- [1] A. S. Ouda, "Development of high-performance heavy density concrete using different aggregates for gamma-ray shielding," *Prog. Nucl. Energy*, vol. 79, pp. 48–55, 2015.
- [2] M. O. Azeez, S. Ahmad, S. U. Al-Dulaijan, M. Maslehuddin, and A. A. Naqvi, "Radiation shielding performance of heavy-weight concrete mixtures," *Constr. Build. Mater.*, vol. 224, pp. 284–291, 2019.
- [3] C. C. Ban *et al.*, "Modern heavyweight concrete shielding: Principles, industrial applications and future challenges; review," *J. Build. Eng.*, vol. 39, p. 102290, Jul. 2021, doi: 10.1016/j.job.2021.102290.
- [4] Z. H. Mahdi, "Effect the addition of MgO powder on some properties of concrete," *J. Eng. Appl. Sci.*, vol. 13, no. 11, pp. 3809–3814, 2018.
- [5] J. Guo, S. Zhang, C. Qi, L. Cheng, and L. Yang, "Effect of calcium sulfoaluminate and MgO expansive agent on the mechanical strength and crack resistance of concrete," *Constr. Build. Mater.*, vol. 299, p. 123833, Sep. 2021, doi: 10.1016/j.conbuildmat.2021.123833.
- [6] C. Du, "A review of magnesium oxide in concrete," *Concr. Int.*, vol. 27, no. 12, pp. 45–50, 2005.
- [7] J. Zhang, "Recent advance of MgO expansive agent in cement and concrete," *J. Build. Eng.*, vol. 45, p. 103633, Jan. 2022, doi: 10.1016/j.job.2021.103633.
- [8] M. Lion, F. Skoczylas, Z. Lafhaj, and M. Sersar, "Experimental study on a mortar. Temperature effects on porosity and permeability. Residual properties or direct measurements under temperature," *Cem. Concr. Res.*, vol. 35, no. 10, pp. 1937–1942, Oct. 2005, doi: 10.1016/j.cemconres.2005.02.006.
- [9] N. Singh, A. Singh, N. Ankur, P. Kumar, M. Kumar, and T. Singh, "Reviewing the properties of recycled concrete aggregates and iron slag in concrete," *J. Build. Eng.*, vol. 60, p. 105150, Nov. 2022, doi: 10.1016/j.job.2022.105150.
- [10] M. U. Khan, S. Ahmad, A. A. Naqvi, and H. J. Al-Gahtani, "Shielding performance of heavy-weight ultra-high-performance concrete against nuclear radiation," *Prog. Nucl. Energy*, vol. 130, p. 103550, Dec. 2020, doi: 10.1016/j.pnucene.2020.103550.
- [11] R. Farokhzad, A. Dadashi, and A. Sohrabi, "The effect of ferrophosphorus aggregate on physical and mechanical properties of heavy-weight

- concrete," *Constr. Build. Mater.*, vol. 299, p. 123915, Sep. 2021, doi: 10.1016/j.conbuildmat.2021.123915.
- [12] Y. Cui, H. Wang, K. Liu, and Q. Wang, "Rheological, deformation behaviors and mechanical changes of MgO-containing concretes with different strength," *J. Build. Eng.*, vol. 64, p. 105593, Apr. 2023, doi: 10.1016/j.jobbe.2022.105593.
- [13] M. A. Abdelgawad, R. M. El Shazly, A. T. M. Farag, I. Adam, and A. M. I. Kany, "Study of mechanical, thermal, and nuclear radiation attenuation properties of tourmaline loaded heavy weight heat resistant concrete as reactor shielding materials," *Prog. Nucl. Energy*, vol. 158, p. 104605, Apr. 2023, doi: 10.1016/j.pnucene.2023.104605.
- [14] R. Joshi, A. Singh, R. Resatoglu, M. Zain, and P. Singh, "Effect of elevated temperature on Portland Pozzolona cement based concrete using Sulphonated naphthalene formaldehyde and Polycarboxylic ether as superplasticizer," *Mater. Today Proc.*, p. S221478532301550X, Mar. 2023, doi: 10.1016/j.matpr.2023.03.483.
- [15] J.-L. Wang *et al.*, "Heavy concrete shielding properties for carbon therapy," *Nucl. Eng. Technol.*, vol. 55, no. 6, pp. 2335–2347, Jun. 2023, doi: 10.1016/j.net.2023.03.003.
- [16] X. Liu, X. Li, Z. Li, X. Wang, Y. Zhang, and N. Wang Supervison, "Influence of heavy concrete on seismic response of transfer and purging rooms of nuclear power plant," *Structures*, vol. 51, pp. 1372–1383, May 2023, doi: 10.1016/j.istruc.2023.03.119.
- [17] M. A. Khalaf, C. C. Ban, and M. Ramli, "The constituents, properties and application of heavyweight concrete: A review," *Constr. Build. Mater.*, vol. 215, pp. 73–89, Aug. 2019, doi: 10.1016/j.conbuildmat.2019.04.146.
- [18] K. Sakr and E. EL-Hakim, "Effect of high temperature or fire on heavy weight concrete properties," *Cem. Concr. Res.*, vol. 35, no. 3, pp. 590–596, Mar. 2005, doi: 10.1016/j.cemconres.2004.05.023.
- [19] M. H. Lai *et al.*, "Effect of fillers on the behaviour of heavy-weight concrete made by iron sand," *Constr. Build. Mater.*, vol. 332, p. 127357, May 2022, doi: 10.1016/j.conbuildmat.2022.127357.
- [20] D. E. Tobbala, "Effect of Nano-ferrite addition on mechanical properties and gamma ray attenuation coefficient of steel fiber reinforced heavy weight concrete," *Constr. Build. Mater.*, vol. 207, pp. 48–58, May 2019, doi: 10.1016/j.conbuildmat.2019.02.099.
- [21] J. Baalamurugan *et al.*, "Recycling of steel slag aggregates for the development of high density concrete: Alternative & environment-friendly radiation shielding composite," *Compos. Part B Eng.*, vol. 216, p. 108885, Jul. 2021, doi: 10.1016/j.compositesb.2021.108885.
- [22] P. Szajerski, J. Celinska, A. Gasiorowski, R. Anyszka, R. Walendziak, and M. Lewandowski, "Radiation induced strength enhancement of sulfur polymer concrete composites based on waste and residue fillers," *J. Clean. Prod.*, vol. 271, p. 122563, Oct. 2020, doi: 10.1016/j.jclepro.2020.122563.

- [23] M. Lardhi and F. Mukhtar, "Radiation shielding performance of seawater-mixed concrete incorporating recycled coarse aggregate and steel slag," *J. Radiat. Res. Appl. Sci.*, vol. 16, no. 1, p. 100528, Mar. 2023, doi: 10.1016/j.jrras.2023.100528.
- [24] D. Józwiak-Niedźwiedzka, M. A. Glinicki, K. Gibas, and T. Baran, "Alkali-Silica Reactivity of High Density Aggregates for Radiation Shielding Concrete," *Materials*, vol. 11, no. 11, p. 2284, Nov. 2018, doi: 10.3390/ma11112284.
- [25] "(PDF) High Density Concrete Incorporating Grit Scale Aggregates for 4th Generation Nuclear Power Plants." [https://www.researchgate.net/publication/357246216\\_High\\_Density\\_Concrete\\_Incorporating\\_Grit\\_Scale\\_Aggregates\\_for\\_4th\\_Generation\\_Nuclear\\_Power\\_Plants](https://www.researchgate.net/publication/357246216_High_Density_Concrete_Incorporating_Grit_Scale_Aggregates_for_4th_Generation_Nuclear_Power_Plants) (accessed Mar. 18, 2023).
- [26] A. Poorarbabi, M. Ghasemi, and M. Azhdary Moghaddam, "Concrete compressive strength prediction using non-destructive tests through response surface methodology," *Ain Shams Eng. J.*, vol. 11, no. 4, pp. 939–949, Dec. 2020, doi: 10.1016/j.asej.2020.02.009.
- [27] Iman. M. Nikbin *et al.*, "Effect of high temperature on mechanical and gamma ray shielding properties of concrete containing nano-TiO<sub>2</sub>," *Radiat. Phys. Chem.*, vol. 174, p. 108967, Sep. 2020, doi: 10.1016/j.radphyschem.2020.108967.
- [28] "Heavyweight Concrete: Measuring, Mixing, Transporting, and Placing - Google Books." [https://books.google.com.pk/books/about/Heavyweight\\_Concrete.html?id=XxwoYAAACAAJ&redir\\_esc=y](https://books.google.com.pk/books/about/Heavyweight_Concrete.html?id=XxwoYAAACAAJ&redir_esc=y) (accessed Jun. 11, 2023).
- [29] D. Józwiak-Niedźwiedzka, K. Gibas, A. M. Brandt, M. A. Glinicki, M. Dąbrowski, and P. Denis, "Mineral Composition of Heavy Aggregates for Nuclear Shielding Concrete in Relation to Alkali-silica Reaction," *Procedia Eng.*, vol. 108, pp. 162–169, 2015, doi: 10.1016/j.proeng.2015.06.132.
- [30] "American Standard ASTM C150 Type1 Specification for Portland Cement." <http://www.tigercement.com/cement-products/ordinary-portland-cement/american-standard-astm-c-150-type-1/> (accessed Mar. 18, 2023).
- [31] "Physical & Chemical Properties Of Cement - [Civil Planets]." <https://civilplanets.com/properties-of-cement/> (accessed Jun. 07, 2023).
- [32] "Standard Specification for Concrete Aggregates." [https://www.astm.org/c0033\\_c0033m-18.html](https://www.astm.org/c0033_c0033m-18.html) (accessed Mar. 18, 2023).
- [33] "C637 | PDF | Construction Aggregate | Concrete." <https://www.scribd.com/document/315322688/C637> (accessed Mar. 18, 2023).
- [34] "ASTM C638-20 - Standard Descriptive Nomenclature of Constituents of Aggregates for Radiation-Shielding Concrete." <https://webstore.ansi.org/standards/astm/astmc63820> (accessed Mar. 18, 2023).



- [35] “ASTM C143/C143M-20 Section 7 Microlearning.” <https://www.astm.org/astm-tpt-591.html> (accessed Mar. 18, 2023).
- [36] “ASTM C948-81(2000) - Standard Test Method for Dry and Wet Bulk Density, Water Absorption, and Apparent Porosity of Thin Sections of Glass-Fiber Reinforced Concrete.” <https://webstore.ansi.org/standards/astm/astmc948812000> (accessed Jun. 07, 2023).
- [37] “ASTM C39/C39M-15a - Standard Test Method for Compressive Strength of Cylindrical Concrete Specimens.” <https://webstore.ansi.org/standards/astm/astmc39c39m15a> (accessed Mar. 18, 2023).
- [38] K. Singh, S. Singh, A. S. Dhaliwal, and G. Singh, “Gamma radiation shielding analysis of lead-flyash concretes,” *Appl. Radiat. Isot.*, vol. 95, pp. 174–179, Jan. 2015, doi: 10.1016/j.apradiso.2014.10.022.
- [39] T. Tuğrul, “Investigation of mass attenuation coefficients, effective atomic numbers, and effective electron density for some molecules: study on chemotherapy drugs,” *J. Radiat. Res. Appl. Sci.*, vol. 13, no. 1, pp. 758–764, Jan. 2020, doi: 10.1080/16878507.2020.1838040.
- [40] “Influence of aggregate characteristics on workability of superworkable concrete | SpringerLink.” <https://link.springer.com/article/10.1617/s11527-015-0522-9> (accessed Jun. 07, 2023).
- [41] M. Shoaib and A. Sardar, “PHYSICAL, MECHANICAL, AND NON-DESTRUCTIVE EVALUATION OF GRIT IRON SCALE HEAVY-DENSITY CONCRETE”.
- [42] B. Fernandes, A. M. Gil, F. L. Bolina, and B. F. Tutikian, “Microstructure of concrete subjected to elevated temperatures: physico-chemical changes and analysis techniques,” *Rev. IBRACON Estrut. E Mater.*, vol. 10, no. 4, pp. 838–863, Aug. 2017, doi: 10.1590/s1983-41952017000400004.
- [43] “Frontiers | Development of high-temperature heavy density dolerite concrete for 4th generation nuclear power plants.” <https://www.frontiersin.org/articles/10.3389/fmats.2023.1057637/full> (accessed Jun. 07, 2023).
- [44] C. Thomas, J. Rico, P. Tamayo, F. Ballester, J. Setién, and J. A. Polanco, “Effect of elevated temperature on the mechanical properties and microstructure of heavy-weight magnetite concrete with steel fibers,” *Cem. Concr. Compos.*, vol. 103, pp. 80–88, Oct. 2019, doi: 10.1016/j.cemconcomp.2019.04.029.
- [45] E. Horszczaruk, P. Sikora, and P. Zaporowski, “Mechanical Properties of Shielding Concrete with Magnetite Aggregate Subjected to High Temperature,” *Procedia Eng.*, vol. 108, pp. 39–46, 2015, doi: 10.1016/j.proeng.2015.06.117.
- [46] “(PDF) Behaviour of cement concrete at high temperature.” [https://www.researchgate.net/publication/237857451\\_Behaviour\\_of\\_cement\\_concrete\\_at\\_high\\_temperature](https://www.researchgate.net/publication/237857451_Behaviour_of_cement_concrete_at_high_temperature) (accessed Jun. 07, 2023).

